

A RESEARCH PROGRAM FOR IMPROVING HEAT TRANSFER PREDICTION CAPABILITY FOR THE LAMINAR TO TURBULENT TRANSITION REGION OF TURBINE VANES/BLADES

Frederick F. Simon
National Aeronautics and Space Administration
Lewis Research Center
Cleveland, Ohio 44135

SUMMARY

A program sponsored by the National Aeronautics and Space Administration (NASA) for the investigation of the heat transfer in the transition region of turbine vanes and blades with the objective of improving the capability for predicting heat transfer is described. The accurate prediction of gas-side heat transfer is important to the determination of turbine longevity, engine performance, and developmental costs. The need for accurate predictions will become greater as the operating temperatures and stage loading levels of advanced turbine engines increase. The present methods for predicting transition shear stress and heat transfer on turbine blades are based on incomplete knowledge and are largely empirical. To meet the objective of the NASA program, a team approach consisting of researchers from government, universities, a research institute, and a Small Business is presented. The research is divided into the areas of experiments, direct numerical simulations (DNS), and turbulence modeling. A summary of the results to date is given for the above research areas in a high-disturbance environment (bypass transition) with a discussion of the model development necessary for use in numerical codes.

INTRODUCTION

A NASA program is described and a progress report is given for the investigation of the heat transfer in the transition region of turbine vanes and blades. The objective of the program is to improve the capability for predicting the gas-side heat transfer for turbine vanes and blades. An improvement in the present predictive accuracy for the heat transfer coefficient from ± 35 to ± 10 percent would significantly improve the ability to predict blade metal temperatures (Stepka, 1980). According to Graham (1979) an error of 35 percent in the heat transfer coefficient is equivalent to about a 100 °F error in wall temperature prediction which can result in an order of magnitude error in the estimated life of a turbine blade. In addition, an inability to accurately predict gas-side heat transfer often leads to an over-design for thermal protection with an increase in the use of coolant air which penalizes propulsion efficiency.

The prediction of heat transfer on a turbine blade or vane is a formidable task due to the flow of high temperature combustion gases with turbulence intensities that range from 10 to 20 percent over curved surfaces that experience favorable and adverse pressure gradients. A research program in transition must consider and evaluate the effects of free-stream turbulence, convex and concave curvature, favorable and adverse pressure gradient, roughness, wake passing, and the stagnation region (fig. 1). A significant portion of the turbine blade/vane may be in a transitional flow between laminar and turbulent boundary layer states. Heat transfer levels in the turbulent flow region of the blade/vane can be as high as three times that of the laminar flow region. Because of the complexity of the problem a program plan was developed at NASA Lewis in 1986 with emphasis on subsonic flows. The NASA Transition Workshop of 1984 (Graham, 1985) formed the basis for the development of this plan. The plan took the approach of initiating the experimental and analytical research with a simple geometry of a flat plate at a zero pressure gradient and systematically increasing the geometry and flow complexities with an eventual effort of a turbine vane in an environment of high turbulence with and without wakes.

The knowledge base is limited for the situation of transition in an engine environment where disturbance levels are initially large. In such a large disturbance environment, traditional linear mechanisms are bypassed and finite nonlinear effects must be considered. This is demonstrated by using the work of Suder, O'Brien, and Reshotko (1988) to make a comparison between the onset of transition for a linear and a nonlinear path (fig. 2). In figure 2, time traces of flush-mounted hot films are shown for cases of low and higher free-stream turbulence intensities. The low free-stream turbulence case shows the presence and amplification of Tollmien-Schlichting (T-S) waves as the path to the onset of transition. The higher free-stream turbulence case shows the sudden appearance of turbulence spots without a sign of linear disturbance growth (although they may be present). As first indicated by Morkovin (1978) the linear stability mechanisms are bypassed and finite nonlinear instabilities occur. Morkovin labels this path to transition as bypass transition. In the bypass model, amplification of Tollmien-Schlichting waves may still be present, but at a much slower rate than the bypass mechanism, and, thus, is of little effect.

The present paper presents the approach in which the NASA Bypass Transition Program proposes to accomplish the stated objective of improved heat transfer prediction capability for the transition region of turbine vanes/blades and a status report of some of the results to date with recommendations for future work. To meet the objective requires that the physics associated with bypass transition heat transfer be investigated, identified, and modeled. The results obtained to date are given in terms of their application to the prediction of transition onset and transition path, as well as through transition skin-friction and heat transfer predictions. Research results are presented in the three areas of experiments, direct numerical simulation (DNS), and turbulence modeling.

NOMENCLATURE

| | |
|-----------------|---|
| C_f | skin friction coefficient |
| H | boundary layer shape factor |
| h | heat transfer coefficient, $W/m^2, K$ |
| K | pressure gradient parameter, $(\nu/U_e)\partial U_e/\partial x$ |
| L_{tr} | transition length |
| N | nondimensional spot formation rate |
| Re_x | Reynolds number based on distance x from leading edge |
| Re_θ | momentum thickness Reynolds number |
| $Re_{\Delta 2}$ | enthalpy thickness Reynolds number |
| St | Stanton number |
| Tu | turbulence intensity at free-stream |
| U_e | free-stream velocity |
| U_τ | friction velocity |

| | |
|-------------|--|
| u',v',w' | fluctuating velocities in x,y,z directions |
| u^+ | streamwise mean velocity in wall units |
| x | distance from leading edge |
| y^+ | normalized y distance in wall units |
| α | spreading angle of spot |
| β | velocity of center of spot divided by free-stream velocity |
| γ | intermittency |
| δ | boundary layer thickness |
| δ^* | displacement thickness |
| η | Blasius similarity variable |
| θ | boundary layer momentum thickness |
| ν | kinematic viscosity |
| Subscripts: | |
| tr | transition onset |
| E | transition end |

APPROACH

It is believed that a team approach will best meet the needs of a fundamental investigation into bypass transition. Simoneau (1986) states that research of a complex nature requires focus and organization and recommends the use of research technology teams. The team members outlined in figure 3 consists of researchers from NASA Lewis, the Center for Modeling of Turbulence and Transition (CMOTT), NASA Ames, NASA Langley, The University of Minnesota, The University of Texas at Austin, Texas A&M, Case Western Reserve University, The University of Toledo, and Dynaflo, Inc. The results of the team efforts in the three areas of experiments, DNS and turbulence modeling are reviewed at annual contractor/grantee workshops sponsored by NASA Lewis.

Experiments on flat surfaces, curved surfaces, and airfoil shapes with and without simulated rotor wakes are being carried out in a number of facilities (figs. 4 to 7). Figure 4 shows the NASA Lewis closed circuit wind tunnel for flat surfaces with variable free-stream turbulence levels and pressure gradient. Measurement systems for this facility allow for characterization of the free-stream intensity and length scale, boundary layer mean temperature and velocity measurements, boundary layer temperature and velocity fluctuations, boundary layer turbulent streamwise and cross-stream stresses and heat fluxes, intermittency and mean surface heat transfer. These same measurements are made for a curved surface in the University of Minnesota test facility (fig. 5). Details of these facilities and measurement approaches may be found in the references of Suder, O'Brien, and

Reshotko (1988); Sohn and Reshotko (1991); Kim and Simon (1991); and in an excellent summary of bypass transition experimental results by Volino and Simon (1991). Measurements of the effects of wakes on transition is being accomplished by using a squirrel cage wake generator at Texas A&M (fig. 6(a)) and the Spoked Wheel Rotor Simulator at NASA Lewis (fig. 6(b)). Transition heat transfer measurements are being made at NASA Lewis on a large blade sprayed with liquid crystals to obtain temperature distributions (fig. 7). Measurements from the above experiments are providing benchmark data for investigation of fundamental mechanisms for model development, and to check numerical predictions.

DNS analyses of a flat surface and an airfoil shape are being made at NASA Ames, NASA Langley, and NASA Lewis. The resulting information provides a numerical data base for modeling and investigating mechanisms. The experimental data generated in the program help to validate the DNS results. Parabolized Stability Equations (PSE) methods are being developed by Dynaflow, Inc. to analyze transition and heat transfer in flows over gas turbine blades.

Turbulence models are being developed at The University of Texas at Austin, Case Western Reserve University, and NASA Lewis for the numerical prediction of transition heat transfer. The development and assessment of these models are being guided by the experimental and DNS results.

RESULTS

A summary of the results to date are presented with emphasis on their application to the understanding and prediction of transition onset and the transition region and the comparison of predictions with benchmark experimental data.

TRANSITION ONSET

Fundamentally, the onset of the transition region is characterized by the intermittent appearance of turbulent spots. These spots grow as they move downstream and eventually merge to form the turbulent boundary layer. This event will have a different observed effect on the physics of flow, the skin friction, and the heat transfer, resulting in different definitions for transition onset. Suder, O'Brien, and Reshotko (1988) experimentally investigated several methods for determining the onset of transition on flat unheated surfaces for a range of free-stream turbulence from 0.3 to 5 percent. The methods for determining transition may be classified into two categories; (1) those based on the physics of flow dynamics and (2) those which result from measurements of skin friction or heat transfer. Methods which fall into the category of flow dynamics are the mean profiles, shape factor, RMS profiles, and the intermittency. Table I lists the five methods (according to the parameters interrogated) employed with a comparison of distances from the leading edge to onset of transition. Mean boundary layer velocity profiles were measured and compared to classical laminar and turbulent profiles. A comparison of the mean profiles with the Blasius profile for a laminar boundary layer (fig. 8(a)) allows one to determine deviation from the Blasius profile as one means of identifying transition onset. For the grid 1 case of figure 8(a), deviation has already begun at 10 in. Another means of onset determination is the deviation of the shape factor from its Blasius value of 2.59 to a decreasing value as the boundary layer becomes more turbulent. A comparison of the boundary layer shape factor variation for four turbulence generating grids is shown in figure 8(b). For the grid 1 case deviation of the shape factor from the traditional laminar value begins at a distance of about 11 in. A more traditional approach for determining onset is based on the distribution of skin friction versus distance as shown in figure 8(c). A comparison of the skin friction coefficient with its theoretical laminar value as shown in figure 8(c) allowed a determination of onset as departure from the laminar line, which for grid 1 is about 9 in. from the plate leading edge. The rms of longitudinal velocity fluctuations is another indicator of transition onset since the velocity fluctuations in a laminar boundary layer are much less

than those obtained for a turbulent boundary layer. The rms profiles of the longitudinal velocity fluctuations (fig. 8(d)) indicate that as the flow begins to transition, the rms values of the velocity fluctuations begin to increase rapidly. In the case of grid 1 (fig. 8(d)) onset begins at approximately 9 in.

The intermittency factor is defined as the percent of time the boundary layer is turbulent and is therefore a measure of the passage of turbulent spots. Therefore, measurement of the intermittency factor should produce the most definitive indication of transition onset. The results presented by Suder, O'Brien, and Reshotko (1988) of flush-mounted hot-films permitted a determination of the intermittency factor as a function of Reynolds number (fig. 8(e)). Transition onset was determined by the location of the hot-film which first recorded intermittency. For grids 0.5 and 1, onset positions of 6.2' and 4.2 in., respectively, were obtained. In the case of grids 2 and 3, transition onset occurred before the location of the first hot-film (4.22 in.). Based on a comparison of the above methods, Suder, O'Brien, and Reshotko (1988) concluded that the intermittency approach gave the earliest indication of transition (table I), suggesting that the other approaches, given above, are not affected by the presence of small amounts of turbulent spots. The five methods of table I show general agreement with each other and show reasonable comparison with the empirical correlations of Van Driest and Blumer (1963), Seyb (1972), Abu-Ghannam and Shaw (1980) and Dunham (1972). Suder, O'Brien, and Reshotko (1988) also noted that, in addition to the influence of free-stream turbulence on transition, there may also be an influence of the frequency distribution (or, alternatively, length scale distribution) of the free-stream disturbances.

As indicated above, onset of transition as determined by the first appearance of turbulent spots is best described by intermittency measurements. An accurate measurement for small values of intermittency is not practical so that use of the extrapolation method of Narashimha (1957) is recommended. Simon and Stephens (1991) used this method to determine the zero intermittency point and the transition length (fig. 9) for the experimental data of Sohn and Reshotko (1991). Volino and Simon (1991) used this approach on the accelerated transition flow data of Blair and Anderson (1987). The results (fig. 10) indicate a change in slope at the lower free-stream turbulence for a value of the function plotted on the ordinate of figure 10 of less than 0.3. Narasimha (1985) and Blair and Anderson (1987) referred to this change in slope as a "subtransition."

Stuckert and Herbert (1992) compared their Parabolized Stability Equations (PSE) approach with the experimental data of Sohn and Reshotko (1991) as shown in figure 11. The onset of transition as defined by the minimum Stanton number is predicted very well by the PSE method. Volino and Simon (1991) compared the zero intermittency point with the minimum Stanton number (used by some as a definition for transition onset) and determined that the minimum Stanton number is located somewhat downstream of the zero intermittency point. This was also noted by Simon and Stephens (1991).

Use of two-equation near-wall turbulence models has in general been successful in the prediction of bypass transition onset. Simon and Stephens (1991) used the Jones-Launder turbulence model to predict onset and compared their results with experimental data and the correlation of Abu-Ghannan and Shaw (1980). The comparison of their results with the correlation of Abu-Ghannan and Shaw is good as shown in figure 12. Simon and Stephens (1991) assumed the transition onset to occur when the numerical computations indicated a rapid increase in turbulence kinetic energy, indicating a nonzero intermittency. This assumption was confirmed (Simoneau and Simon, 1993) by comparison with the DNS calculations of Rai and Moin (1991) shown in figure 13 for the case of zero pressure gradient and 2.6 percent free-stream turbulence. Figure 13 shows how the two-equation turbulence model captures the nonlinear disturbance growth which leads to the first sign of turbulent spot formation. Suder, O'Brien, and Reshotko's (1988) single-wire measurements within the boundary layer indicated spot initiation at a boundary layer turbulence level of 3.5 percent regardless of the path to transition (high or low free-stream turbulence). This experimental result appears consistent with the calculations of Simon and Stephens (1991) and Rai and Moin (1991) shown in figure 13.

Figure 13 suggests that, below a certain critical Reynolds number, amplification of disturbances is not significant. This was the basis for the assumption made by Schmidt and Patankar (1988) in their development of a turbulence model for transition and the basis used by Simon and Stephens (1991) for initializing the calculations for disturbance energy shown in figure 13. The assumption made by the above authors was that this critical Reynolds number is close to the critical Reynolds number for linear instability. To help establish the credibility of this assumption, DNS studies of controlled disturbances in a Blasius boundary layer are being performed at NASA Lewis using Spalart's fringe code (Ashpis and Spalart, 1992, and Ashpis and Spalart, 1993). The objective of these studies is to simulate bypass mechanisms by introducing into the boundary layer controlled discrete disturbances and computing the space-time evolution of the resulting disturbances and their spectra. The input disturbances are of linear and nonlinear amplitudes, and are introduced at subcritical and supercritical Reynolds numbers. An example of a response to a pulsed disturbance is given in figure 14, which shows a structure composed of a nonlinearly distorted wave packet superposed on a narrow, streamwise elongated, structure. Wave packets may develop in various routes, one of which is into turbulent spots.

Other experimental and analytical values for transition onset are given in figure 12. Figure 12 shows some experimental transition onset results given in the survey report of Volino and Simon (1991) and some examples of the result of transition onset calculations utilizing a number of turbulence models developed at the University of Texas at Austin. Figure 12 shows the general applicability of turbulence models for predicting transition onset. Turbulence models developed at the University of Texas at Austin (Crawford, 1991) called the Texas model (TXM) and the Multi-Time-Scale (MTS) model have the potential of improved simulation of the transition region.

The K.Y. Chien turbulence model (1982) results shown in figure 12 were found by Stephens and Crawford (1990) to give a premature value for transition onset. They explained that this is because the damping function of the Chien model is dependent only on the boundary layer normal distance and that an improved onset prediction is obtained when the damping function is dependent on the turbulent Reynolds number. The inability of the K.Y. Chien model to simulate transition onset was also found by the heat transfer Navier-Stokes calculations of a turbine blade by Ameri and Arnone (1992).

The effect of curvature on transition onset at low free-stream turbulence is summarized from the experimental work of Wang (1984) and Kim and Simon (1991) in figure 15. As indicated in figure 15, a convex surface when compared to a flat surface will delay transition onset and a concave surface compared to a flat surface will shift transition onset upstream. The differences in onset location, based on the minimum in the Stanton number, for a convex surface and a flat surface diminish as the free-stream turbulence increases (fig. 16).

TRANSITION REGION

This section describes the relevant physical characteristics of the transition region required for the understanding and modeling of the region. Figure 17 shows conditionally sampled velocity profiles in the transition region of a flat plate as reported by Sohn, Reshotko, and Zaman (1991). Figure 17 shows the departure from a Blasius profile as an indication of the transition region which occurs after transition onset. The nonturbulent profiles increase in their deviation from the Blasius curve with increases in intermittency. With increase in intermittency the turbulent part of each profile is seen to become more like that of a fully-turbulent boundary layer. The effect of the nonturbulent profiles showing increased deviation from a Blasius profile with increased intermittency is attributed by Kim and Simon (1991) and Sohn and Reshotko (1991) to a post-burst relaxation period required for a disturbance in the nonturbulent part of the flow to damp-out. With an increase in the number of turbulent spots, or increased intermittency, there are more post-burst relaxation periods included in the nonturbulent part of the flow. Figure 17 demonstrates that the transition region cannot be accurately

described by a combination of Blasius and fully turbulent boundary layer profiles as proposed by Dhawan and Narasimha (1958) by using an intermittency weighting approach.

As can be observed in figure 8(d), the streamwise component of turbulence intensity measurements will, under certain conditions, exhibit a double hump. The observance of a double hump in the data is attributed to the switching between laminar and turbulent boundary layer flows as a turbulent spot goes by a hot-wire probe. Confirmation of this switching explanation is seen in the DNS calculations of the streamwise fluctuation of Rai and Moin (1991) which do not exhibit a double hump (fig. 18). This switching effect gives rise to a velocity fluctuation level which is higher than that obtained in either the laminar or the turbulent regions and affects the experimental shear stress profile (Kim and Simon, 1991).

It is generally known that a concave curvature has a destabilizing effect on flow, with transition occurring earlier than on a flat plate. Görtler vortices are the primary mode of instability. Kim and Simon (1991) established the existence of stable vortices on a concave surface for low free-stream turbulence, but found no stable vortices for a higher turbulence intensity case (8.3 percent). Figure 19 displays Stanton number results obtained at the University of Minnesota (Volino and Simon, 1993). They show the effects of concave curvature and acceleration as compared to unaccelerated flow on a flat plate. The unaccelerated, flat plate, 8 percent free-stream turbulence data (Kim and Simon, 1991) are only slightly above a standard, fully-turbulent flow, flat-plate, low turbulence intensity correlation, which is shown in figure 19 for reference. Unaccelerated flow, concave wall data taken at 8 percent free-stream turbulence intensity lie well above this correlation. Accelerated concave wall data fall below the correlation as do accelerated flat plate data of Blair and Anderson (1987). The accelerated flat plate data taken at 5 percent turbulence intensity show a transition from the laminar to turbulent flow; however, there is no sign of transition for any of 8 percent turbulence intensity cases, even the accelerated-flow cases. On the concave surface, acceleration lowers the Stanton number in opposition to the curvature effect. This countering of the curvature effect by acceleration was also seen in the measurements of the shear stress profiles obtained at the University of Minnesota; figure 20, where acceleration counteracts the concave curvature effects, reducing the shear stress profile to unaccelerated flat-wall levels. Increasing the acceleration is expected to further reduce the level of shear stress. The above mentioned effects of free-stream turbulence, curvature, and acceleration lend further understanding of the highly-disturbed flow and will play an important role in the development of predictive models.

Experimental and calculated values of the momentum thickness Reynolds number at the onset and end of transition, as compared with the correlations of Abu-Ghannam and Shaw (1980), are given in figures 12 and 21. In these plots, the transition region may be defined as existing between an intermittency of 0 and 0.99 or between the points of minimum and maximum heat transfer. These curves present a good summary of the measurements and calculations for the transition region. These curves demonstrate the strong effect free-stream turbulence intensity plays, although it is expected that the spectra and length scale of the free-stream turbulence will be needed to further refine the turbulence effects.

As indicated above, the use of low Reynolds number, two-equation turbulence models (figs. 12 and 21) appears to have some success in simulating transition onset and end which is governed by the transport and production of turbulence in the boundary layer. Generally, as can be seen in figure 21, these models give an underprediction of transition length. A reason for this may be found in the work of Volino and Simon (1993). Volino and Simon (1993) applied an octant analysis to the experimental data to analyze the difference in structure between turbulent and transitional flows. They indicate that transitional boundary layers show incomplete mixing or incomplete development of turbulence with a domination of the large scale eddies. This is attributed to the incomplete development of the cascade of energy from large to small scales. Based on this observation, it is stated that the standard k - ϵ turbulence model does not comprehend the physics of the transition region and what is needed is a model that will comprehend both large and small scales separately. This would require a modified k - ϵ equation with perhaps two equations for the turbulent kinetic energy (k); one equation for

the large scale eddies and one for the small scale eddies. Such a multi-time-scale (MTS) model for application to transition flows has been implemented by Crawford (1992). This model is an evolution of two-scale $k-\epsilon$ models developed by Hanjalic, Launder, and Schiestel (1980) and Kim (1990). A preliminary result (fig. 21) shows promise for this MTS model's ability to simulate the transition region for turbulence levels greater than 2 percent.

Schmidt and Patankar (1988) attributed the underprediction of the transition length to the production term of the turbulent kinetic energy equation. They modified the production term to make predictions consistent with experimental results. Figure 22 shows the effect of the modification as compared with the Abu-Ghannam and Shaw (1980) correlations.

Simon and Stephens (1991), following the concept of Schmidt and Patankar, utilized stability considerations for determining the location of the initial profiles in the numerical calculations, and developed a basis for utilizing intermittency in transition calculations. They followed the method of Vancoille and Dick (1988) to develop conditional averaged turbulence model equations for heat transfer. This approach is felt to be better than a global time average approach which does not take into account a transition zone which consists of turbulent spots surrounded by laminar-like fluid. The method of Simon and Stephens (1991) assumes the universal intermittency relationship of Narasimha (1957) which compares favorably with the experimental data as presented by Volino and Simon (1991). As can be seen on figure 23 a determination of intermittency requires knowledge of the transition length. This was done by Simon and Stephens by utilizing the approach of Narasimha (1985) which expresses the transition length in terms of a nondimensional spot formation rate (N). Narasimha (1985) demonstrates that N reaches a constant value at the higher turbulence levels. Figure 24 gives the value of N used by Simon and Stephens which is based on experiment. The value of N given in figure 24 may be compared to the result of an analysis by Simon (1994). The analytical value of N reported by Simon is a constant of 0.00029, in agreement with the experimental data of figure 24 and in accordance with the analysis dependent on turbulent spot characteristics. The use of N permits a determination of transition length by means of the following equation reported by Simon and Stephens (1991):

$$Re_{L_{tr}} = \frac{2.15}{\sqrt{N}} Re_{\theta_r}^{3/2} \quad (1)$$

Transition calculations were made by Simon and Stephens (1991) utilizing equation (1) and the intermittency path equation of Narasimha (1957) with the TEXSTAN code of Crawford (1985). Results of calculations employing equation (1) are compared to the experimental results of Volino and Simon (1991, table 5) in figure 25. The experimental data of Kim and Simon (1991), Suder et al. (1988), Sohn and Reshotko (1991), and Kuan and Wang (1990) are for zero-pressure-gradient flow on a flat plate. The data of Blair and Anderson (1987) is for two flat plate data sets with two values of acceleration. In general, there is a good relationship with equation (1) and the experimental data with the exception of the higher acceleration data. With an increase in flow acceleration there is an apparent increase in transition length. This increase in transition length is consistent with the characteristics of turbulent spots under accelerating conditions as shown by Simon (1994). Simon using the Narasimha (1985) reported results of Wyganaski (1981), which show a low turbulent spot spreading angle of 5 degrees for a favorable pressure gradient case, calculates a value of N given in figure 25. The results of the numerical calculations utilizing the TEXSTAN code are given in figure 26 for cases computed with and without intermittency. The value of using intermittency for improvement of the transition model is clearly demonstrated. It is interesting to note, according to the calculations, that the boundary layer acts as if it were a laminar boundary layer up to a significant value of the intermittency. This is consistent with the measured velocity profiles of Sohn, O'Brien, and Reshotko (1989) which showed a laminar-like overall profile in the transition region for intermittency value up to 0.34 at 1 percent free-stream turbulence.

EXAMPLES OF COMPUTATIONAL RESULTS

Some examples of computations compared to experimental data are presented here as a means of demonstrating "the bottom line" objective of successfully predicting bypass transition heat transfer.

A DNS calculation of transition on a flat plate, for a free-stream turbulence and velocity of 2.6 percent and 100 ft/s, was performed by Rai and Moin (1991). Rai and Moin use a high-order-accurate finite-difference approach for the direct numerical simulation of transition and turbulence. Figure 27 compares the experimental results of Suder, O'Brien, and Reshotko (1988) and Sohn and Reshotko (1991) with the numerical results for two computational grid distributions. Sufficient confidence has been established with the DNS approach that the resulting numerical base is seen as valuable for the development and testing of turbulence models applicable to bypass transition.

As explained above, Schmidt and Patankar (1988) modified the production term of the turbulent kinetic energy equation. They referred to this approach by the acronym PTM or Production Term Modification. Figure 28 demonstrates the improved prediction of transition as a result of using PTM. Examples of calculations comparisons with experimental data, as reported by Schmidt and Patankar, are given in figure 29. The comparison with the data of Wang (1984) for a flat plate at 2 percent free-stream turbulence is excellent (fig. 29(a)) and is an improvement over the mixing length approach of Park and Simon (1987). The use of the PTM approach for predicting the flat plate heat transfer data of Rued (1985) for a free-stream turbulence range of 1.7 to 10.8 percent is shown in figure 29(b). A comparison with the C3X blade results of Hylton et al. (1983) is given in figure 29(c). The calculations for figure 29(c) required the modification of the near-wall length scale due to the presence of an adverse pressure gradient on the suction side of the blade. The lower curve for each run shows the effect of the length scale modification. While there is a favorable comparison of the computations with experiment, the accuracy of the prediction in the fully turbulent region diminished as the blade Reynolds number increased.

The use of the intermittency computational approach of Simon and Stephens (1991) has promise for prediction of transitional flows. A comparison with the experimental data of Blair and Werle (1980) is given in figure 30. There is generally good agreement. Figure 30 contrasts the definition of transition onset based on intermittency and the minimum in heat transfer.

At the University of Texas at Austin, a number of turbulence models have been tested for their ability to simulate bypass transition. Examples of results of comparisons with the flat plate experimental heat transfer data of Sohn and Reshotko (1991) and the benchmark skin friction data set of the European ERCOFTAC conference, coordinated by Savill (1991), are given in figures 31 and 32. At a free-stream turbulence level of 3 percent, the experimental data of Sohn and Reshotko are best described by the Launder-Sharma (LS) and Texas (TXM) models (Crawford, 1993). There is some confirmation of this in the skin friction coefficient comparison of figure 32 (Crawford, 1992). The Nagano-Tagawa (NT) model also shows some promise. A more critical test of turbulence models for the prediction of the heat transfer on turbine blades was made by Sieger, Schulz, Crawford, and Wittig (1992). An example of their results is given in figure 33. Figure 33 shows that for a free-stream turbulence of 8.3 percent, the heat transfer experimental data of the pressure side of the Hylton et al. (1983) blade is reproduced well by all the models tested. The lowest heat transfer is given by the Launder-Sharma model. The pressure side has a transitional like behavior over the entire surface. For the prediction of transition on the suction side of the blade, figure 33 indicates that improvements are needed in the turbulence models. With the exception of the Launder-Sharma model, all the models give an early transition at the high free-stream turbulence intensity.

The potential of the Launder-Sharma model to simulate transition was further confirmed by the work of Wu and Reshotko (1991) as shown in figure 34. The work of Yang (1991) suggests an improvement over the

Launder-Sharma model by the use of a new low-Reynolds-number turbulence model (Yang and Shih, 1992) and an intermittency weighing factor. The intermittency weighing factor used by Yang is related to an intermittency factor defined by the variation of the boundary layer shape factor through the transition region. The intermittency weighing factor is used to modify the calculated eddy viscosity in the transition region. The result is an improvement over the Launder-Sharma model, as shown in figure 35. In addition, Yang and Shih point out that a drawback of the LS model is its inability to perform as well as other models for fully-developed turbulent boundary layers.

As indicated above a possible improvement to the $k-\epsilon$ turbulence model is the Multi-Time-Scale (MTS) model. A comparison of this model, developed at the University of Texas under the supervision of Crawford (1993), with data set T3A is given in figure 36. Comparing figure 36 with figure 32 shows the potential of the MTS model.

CONCLUDING REMARKS

This progress report of a NASA research program for the prediction of transition heat transfer on turbine vane and blades has demonstrated the value of a team approach with an appropriate experimental and analytical skill mix, as recommended by Simoneau (1986) for complex problems. The synergism resulting from a team of experimentalists, analysts, and modelers is required for the complex research area of bypass transition which requires an in-depth investigation of the effects of free-stream turbulence, convex and concave curvature, favorable and adverse pressure gradient, wakes, and the effect of the stagnation region of a blade or vane. The team effort has led to the following accomplishments:

1. An extensive experimental data base of bypass transition on flat and curved surfaces has been obtained. The detailed nature of the data base permits an investigation of the physics involved and is an aid in the development and testing of turbulence models. Conditional analyses have demonstrated that the transition region is not a simple combination of Blasius and turbulent boundary layer profiles.
2. Effects of convex and concave curvature on transition have been documented. When low free-stream turbulence level cases are compared to the results of transition on a flat surface at equivalent turbulence levels, convex curvature will delay transition onset and concave curvature will shift transition onset upstream.
3. The effect of acceleration and free-stream turbulence for a transitioning boundary layer on a concave surface is being documented. The existence of stable vortices on a concave-curved wall were found at low free-stream turbulence intensities. No coherent vortices were found at the higher free-stream turbulence intensities.
4. Two-equation turbulence models appear to capture the growth of nonlinear disturbances in bypass transition and are capable, with appropriate damping functions and constants, of predicting transition onset. These models under-predict the transition length, however, unless (1) provision is made for the intermittent nature of the transition region, (2) a modification is made for the rate of turbulence production, or (3) a multiscale model is used to account for the incomplete nature of the turbulent energy cascade in the transition region. The need for a multiscale turbulence model has been confirmed by an analysis of the experimental data. A number of low-Reynolds number turbulence models have been assessed. The Launder-Sharma, the Texas and the Yang and Shih turbulence models were found to be effective for simulating bypass transition, although improvements in these models, and all the models tested, are required.
5. Direct Numerical Simulation (DNS) has proven to be a very powerful tool for (1) understanding the physics, (2) supporting and guiding the experimental results, and (3) forming a data base for the development

and testing of transition turbulence models. Results obtained with DNS compare very well to the experimental results.

6. Transition onset was well predicted by the Parabolized Stability Equations (PSE) method. This method has the potential of predicting most of the transition region with reasonable computational requirements.

The following recommendations for future work are based on the annual NASA-Lewis bypass transition workshops:

1. There are indications that spectra and length scales of free-stream turbulence play a role in the transition process. These factors should be investigated. The use of laboratory and DNS numerical experiments would be useful here.

2. Future experiments should better document the free-stream turbulence by providing the three components of velocity fluctuations, the frequency range over which the free-stream turbulence was measured, and other turbulence characteristics.

3. DNS calculations with heat transfer and for a turbine blade geometry should be made. DNS calculations should be applied to the study of boundary layer receptivity to free-stream disturbances and their effect on stability. A DNS data base should be established.

4. A study on the effect of the leading edge geometry on transition, with use of experiments and DNS, should be initiated.

5. There needs to be an increase in the range of the turbulence levels studied (6 to 20 percent), which are more in line with the levels present in a combustor.

6. The community should continue to develop the use of the PSE approach as a design tool.

7. There should be an increase in the experimental Mach number to better simulate actual engine conditions and permit increased computational efficiency of the numerical codes for the purpose of comparison of numerical and experimental results. Also there should be transonic measurements with shock-boundary layer interactions to investigate this effect.

8. The community should continue the development of turbulence models which are more faithful to the physics of transition, as determined by DNS and experimental efforts. Development of multiscale, two-equation turbulence models should continue.

9. The application of Large Eddy Simulation (LES) to bypass transition should be investigated.

10. Spectral measurements within the late transitional boundary layer should be made to determine which wavelengths are amplified and the relationships of these wavelengths to the most unstable wavelengths computed from linear stability theory.

Some of the above recommendations are already being carried out by members of the NASA bypass transition team. In addition, the work on the effect of unsteady flows (e.g., wakes) has been initiated. Significant progress has been made in the understanding and improving predictive capability of heat transfer on turbine vanes and blades. This progress has, to date, been mostly limited to flat and curved surfaces with little work on actual vanes or blades. A key recommendation of the transition team is to increase the effort being made on

vanes and/or blades. This recommendation is consistent with the original plan of 1986 of increasing geometry and flow complexities. We believe we are on schedule.

REFERENCES

- Abu-Ghannam, B.J.; and Shaw, R.: Natural Transition of Boundary Layers—The Effects of Turbulence, Pressure Gradient, and Flow History. *J. Mech. Eng. Sci.*, vol. 22, no. 5, 1980, pp. 213–228
- Ameri, A.A.; and Arnone, A.: Navier-Stokes Turbine Heat Transfer Predictions Using Two-Equation Turbulence Closures. NASA TM-105817, 1992.
- Ashpis, D.E.; and Spalart, P.R.: Direct Numerical Simulation of Wall-Generated Disturbances in a Boundary Layer. *Bull. Am. Phys. Soc.*, vol. 37, 1992, pp. 1813–1817.
- Ashpis, D.E.; and Spalart, P.R.: Work in process, 1993.
- Blair, M.F.: Influence of Free-Stream Turbulence on Turbulent Boundary Layer Heat Transfer and Mean Profile Development, Pt. I. Experimental Data. *J. Heat Transfer*, vol. 105, Feb. 1983, pp. 33–40.
- Blair, M.F.; and Anderson, O.L.: Study of the Structure of Turbulence in Accelerating Transitional Boundary Layers. VTRC Report R87-956900-1, United Technologies Research Center, East Hartford, CT, 1987.
- Blair, M.F.; and Werle, M.J.: The Influence of Free-Stream Turbulence on the Zero Pressure Gradient Fully Turbulent Boundary Layer. UTRC Report R80-914388-12, United Technologies Research Center, East Hartford, CT, 1980.
- Chien, K.-Y.: Predictions of Channel and Boundary-Layer Flows with a Low-Reynolds-Number Turbulence Model. *AIAA J.*, vol. 20, no. 1, 1982, pp. 33–38.
- Coakley, T.J.: Turbulence Modeling Methods for the Compressible Navier-Stokes Equations. AIAA Paper 83-1693, 1983.
- Crawford, M.E.: TEXSTAN Program. University of Texas at Austin, 1985.
- Crawford, M.E.; and Simon, F.F.: Turbulence Modeling for the Simulation of Transition in Wall Shear Flows. Progress Report, NASA Grant NAG3-864, 1991.
- Crawford, M.E.; and Simon, F.F.: Progress Report, NASA Grant NAG3-864, 1992.
- Crawford, M.E.; and Simon, F.F.: Progress Report, NASA Grant NAG3-864, 1993.
- Dhawan, S.; and Narasimha, R.: Some Properties of Boundary Layer Flow During Transition From Laminar to Turbulent Motion. *J. Fluid Mech.*, vol. 3, 1958, pp. 418–436.
- Dunham, J.: Predictions of Boundary Layer Transition on Turbomachinery Blades. *Boundary Layer Effects in Turbomachines*, AGARD AG-164, J. Surugue, ed., 1972.
- Graham, R.W.: Fundamental Mechanisms that Influence the Estimate of Heat Transfer to Gas Turbine Blades. NASA TM-79128, 1979.

- Graham, R.W.: Transition In Turbines. NASA CP-2386, 1985.
- Hanjalic, K.; Launder, B.E.; and Schiestel, R.: Multiple-Time-Scale Concepts in Turbulent Transport Modelling. Vol. 2: Turbulent Shear Flows. Springer-Verlag, New York, 1980.
- Hylton, L.D., et al.: Analytical and Experimental Evaluation of the Heat Transfer Distribution Over the Surfaces of Turbine Vanes. NASA CR-168015, 1983.
- Kuan, C.L.; and Wang, T.: Investigation of Intermittent Behavior of Transitional Boundary Layer Using a Conditional Averaging Technique. Exp. Thermal Fluid Sci., vol 103, 1990, pp. 157-173.
- Kim, S.-W.: Numerical Investigation of Separated Transonic Turbulent Flows With a Multiple-Time-Scale Turbulence Model. NASA TM-102499, 1990.
- Kim, J.; and Simon, T.W.: Free-Stream Turbulence and Concave Curvature Effects on Heated, Transitional Boundary Layers. NASA CR-187150, 1991.
- Launder, B.E.; and Sharma, B.I.: Application of the Energy-Dissipation Model of Turbulence to the Calculation of Flow Near a Spinning Disc. Lett. Heat Mass Transfer, vol 1, 1974, pp. 131-138.
- Morkovin, M.V.: Instability Transition to Turbulence and Predictability. AGARD AG-236, 1978.
- Myong, H.K.; and Kasagi, N.: A New Approach to the Improvement of k- ϵ Turbulence Model for Wall-Bounded Shear Flows, JSME Int. J., Ser. II, vol 33, 1990, pp. 63-72.
- Narasimha, R.: On the Distribution of Intermittency in the Transition Region of a Boundary Layer, J. Aeronaut. Sci., vol. 24, no. 9, 1957, pp 711-712.
- Narasimha, R.: The Laminar-Turbulent Transition Zone in the Boundary Layer. Prog. Aerosp. Sci., vol. 22, 1985, pp 29-80.
- Park, W.; and Simon, T.: Prediction of Convex-Curved Transitional Boundary Layer Heat Transfer Behavior Using MLH Models. Presented at the Joint ASME/JSME Thermal Engineering Conference, Honolulu, HI, March 22-27, 1987.
- Rai, M.M.; and Moin, P.: Direct Numerical Simulation of Transition and Turbulence in a Spatially Evolving Boundary Layer. AIAA Paper 91-1607, 1991.
- Rued, K.: Transitional Boundary Layers Under the Influence Of High Free Stream Turbulence, Intensive wall Cooling and High Pressure Gradients in Hot Gas Circulation. NASA TM-88524, 1985 (Translation of thesis submitted at the University of Karlsruhe, West Germany).
- Savill, A.M.: Turbulence Model Predictions for Transition under Free-Stream Turbulence. Presented at the RAeS Transition and Boundary Layer Conference, Cambridge, England, 1991.
- Schmidt, R.C.; and Patankar, S.V.: Two-Equation Low-Reynolds-Number Turbulence Modeling of Transitional Boundary Layer Flows Characteristic of Gas Turbine Blades. NASA CR-4145, 1988.
- Schubauer, G.B.; and Skramstad, H.K.: Laminar-Boundary Layer Oscillations and Transition on a Flat Plate. NACA Report 909, 1948.

- Seyb, N.J.: The Role of Boundary Layers in Axial Flow Turbomachines and Prediction of Their Effects. *Boundary Layer Effects in Turbomachines*, AGARD AG-164, J. Surugue, ed., 1972, pp. 261-274.
- Shih, T.H.: An Improved κ - ϵ Model for Near-Wall Turbulence and Comparison With Direct Simulation. NASA TM-103221, 1990.
- Sieger, K., et al.: Comparative Study of Low-Reynolds Number k - ϵ Turbulence Models for Predicting Heat Transfer along Turbine Blades with Transition. Presented at: International Symposium on Heat Transfer in Turbomachinery, Athens, Greece, 1992.
- Simon, F.: The Use of Transition Region Characteristics to Improve the Numerical Simulation of Heat Transfer in Bypass Transitional Flows. To be published in 1994.
- Simon, F.F.; and Stephens, C.A.: Modeling of the Heat Transfer in Bypass Transitional Boundary-Layer Flows. NASA TP-3170, 1991.
- Simoneau, R.J.: Opportunities and Challenges in Heat Transfer—From the Perspective of the Government Laboratory. *Heat Transfer Eng.*, vol. 7, nos. 3-4, 1986, pp. 76-81.
- Simoneau, R.J.; and Simon, F.F.: Progress Towards Understanding and Predicting Heat Transfer in the Turbine Gas Path, *Int. J. Heat Fluid Flow*, vol. 14, no. 2, 1993, pp. 106-128. (Also, NASA TM-105674, 1993.)
- Sohn, K.H.; O'Brien J.E.; and Reshotko, E.: Some Characteristics of Bypass Transition in a Heated Boundary Layer. NASA TM-102126, 1989.
- Sohn, K.H.; and Reshotko, E.: Experimental Study of Boundary Layer Transition With Elevated Freestream Turbulence on a Heated Flat Plate. NASA CR-187068, 1991.
- Sohn, K.H.; Reshotko, E.; and Zaman, K.B.M.Q.: Experimental Study of Boundary Layer Transition on a Heated Flat Plate. NASA TM-103779, 1991.
- Sohn, K.H.; Zaman, K.B.M.Q.; and Reshotko, E.: Turbulent Heat Flux Measurements in a Transitional Boundary Layer. NASA TM-105623, 1992.
- Stephens, C.A.; and Crawford, M.E.: An Investigation into the Numerical Prediction of Boundary Layer Transition Using the K.Y. Chien Turbulence Model. NASA CR-185252, 1990.
- Stepka, F.S.: Analysis of Uncertainties in Turbine Metal Temperature Predictions. NASA TP-1593, 1980.
- Stuckert, G.K.; and Herbert, T.: Transition and Heat Transfer in Gas Turbines. Final Report. NASA Contract NAS3-26602, 1992.
- Suder, K.L.; O'Brien, J.E.; and Reshotko, E.: Experimental Study of Bypass Transition in a Boundary Layer. NASA TM-100913, 1988.
- Van Driest, E.R.; and Blumer, C.B.: Boundary Layer Transition: Free-stream Turbulence and Pressure Gradient Effects. *AIAA J.*, vol. 1, no. 6, 1963, pp. 1303-1306.

- Vancoillie, G.; and Dick, E.: A Turbulence Model for the Numerical Simulation of the Transition Zone in a Boundary Layer. *Int. J. Eng. Fluid Mech.*, vol. 1, no. 1, 1988, pp. 28-49.
- Volino, R.J.; and Simon, T.W.: Bypass Transition in Boundary Layers Including Curvature and Favorable Pressure Gradient Effects. NASA CR-187187, 1991.
- Volino, R.J.; and Simon, T.W.: An Application of Octant Analysis to Turbulent and Transitional Flow Data. Presented at the International Symposium on Gas Turbines in Cogeneration, IGTI ASME TURBO EXPO, Cincinnati, OH, May 24-27, 1993.
- Volino, R.J.; and Simon, T.W.: Measurements in a Transitional Boundary Layer on a Concave Surface. Progress Report, NASA Grant NAG3-1249, 1993.
- Wang, T.: An Experimental Investigation of Curvature and Free-free-stream Turbulence Effects on Heat Transfer and Fluid Mechanics in Transitional Boundary Layers. PhD Thesis, Department of Mechanical Engineers, University of Minnesota, MN, 1984.
- Wynanski, I.: The Effects of Reynolds Number and Pressure Gradient on the Transitional Spot in a Laminar Boundary Layer. The Role of Coherent Structures in Modelling Turbulence and Mixing; Proceedings of the International Conference, T. Timencz, ed., Springer-Verlag, Berlin, 1981, pp. 304-332.
- Wu, S.T.; and Reshotko, E.: Environmental Effects on Transition and the Control of Transition. Cooperative Agreement under contract NCC3-124, 1991.
- Yang, Z.: Modeling of Near Wall Turbulence and Modeling of Bypass Transition. Center for Modeling of Turbulence and Transition (CMOTT): Research Briefs, W.W. Liou, ed., NASA TM-105834, pp. 83-94,
- Yang, Z.; and Shih, T.H.: A $k-\epsilon$ Modeling of Near Wall Turbulence. NASA TM-105238, 1991.
- Yang, Z.; and Shih, T.H.: A $k-\epsilon$ Calculation of Transitional Boundary Layers. NASA TM-105604, 1992.

**TABLE I.—SUMMARY OF TRANSITION
ONSET (SUDER, O'BRIEN, AND
RESHOTKO, 1988)**

| Grid | Nominal free-stream turbulence, percent | Method | Onset, in., χ |
|-------------|--|---|--|
| 0 | 0.3 | Mean profiles Shape factor Skin friction RMS profiles Intermittency | 40.3 40.3 38.0 40.0 38.3 |
| 0.5 | 0.7 | Mean profiles Shape factor Skin friction RMS profiles Intermittency | 9.3 9.3 9.3 8-9 6.2 |
| 1 | 1 | Mean profiles Shape factor Skin friction RMS profiles Intermittency | 9-10 11 9 9 4.2 |
| 2 | 2 | Mean profiles Shape factor Skin friction RMS profiles Intermittency | <5 <5 <5 <5 <4 |

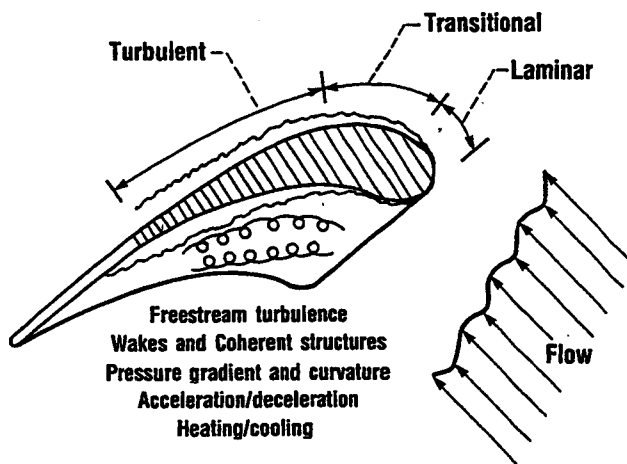


Figure 1.—Working environment of turbine vanes/blades.

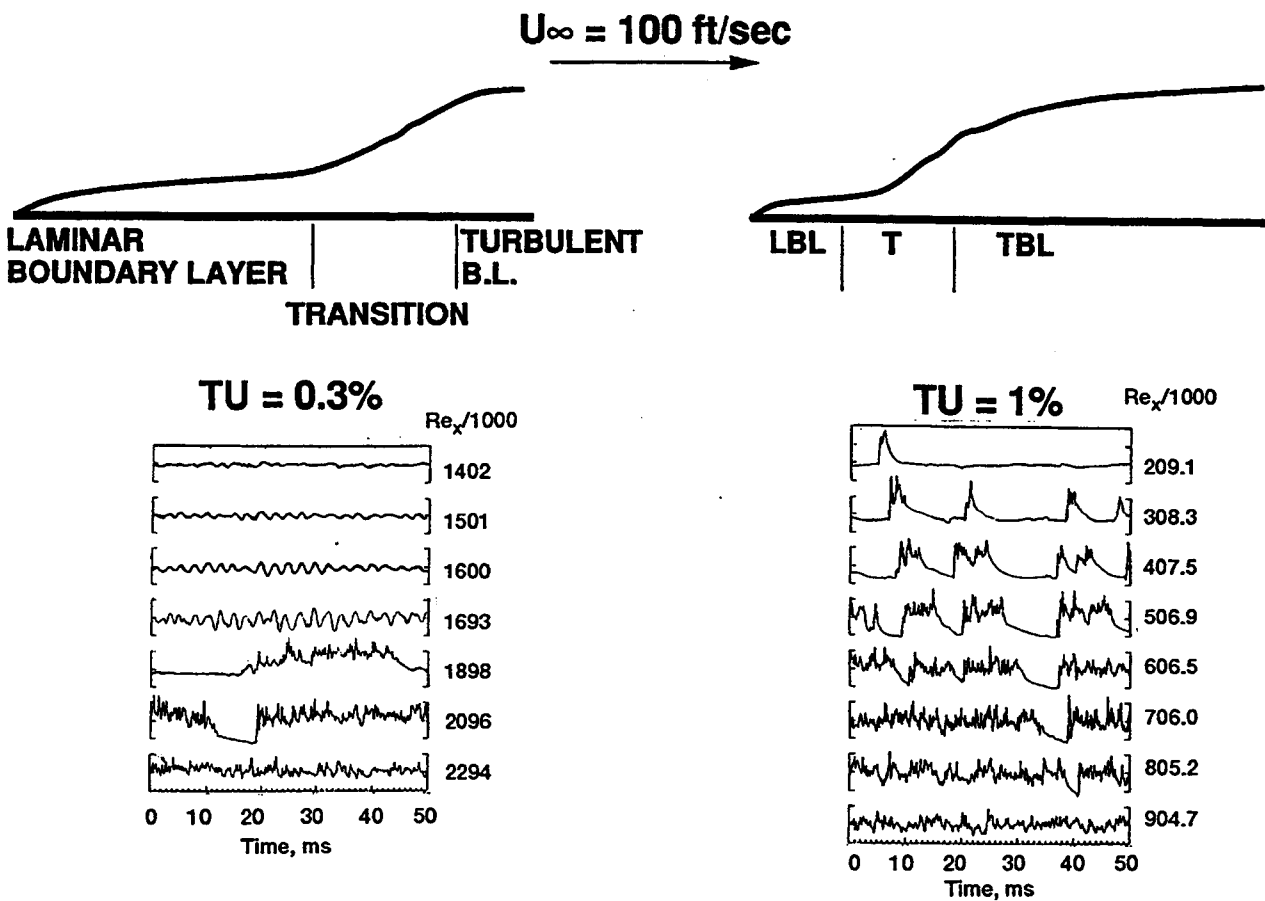


Figure 2.—Linear versus bypass path to transition. From Suder, O'Brien, Reshotko (1988).

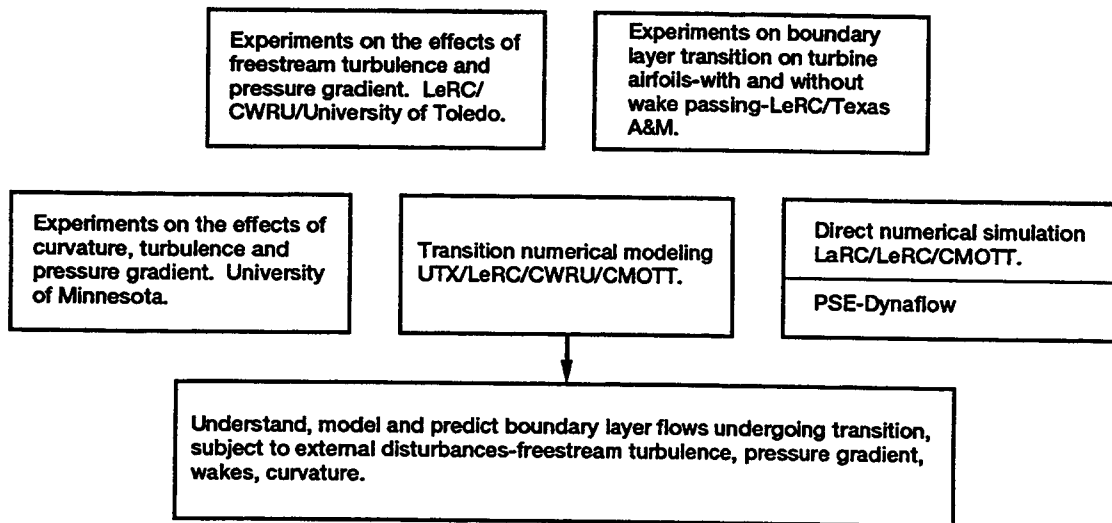


Figure 3.—By-pass transition research program.

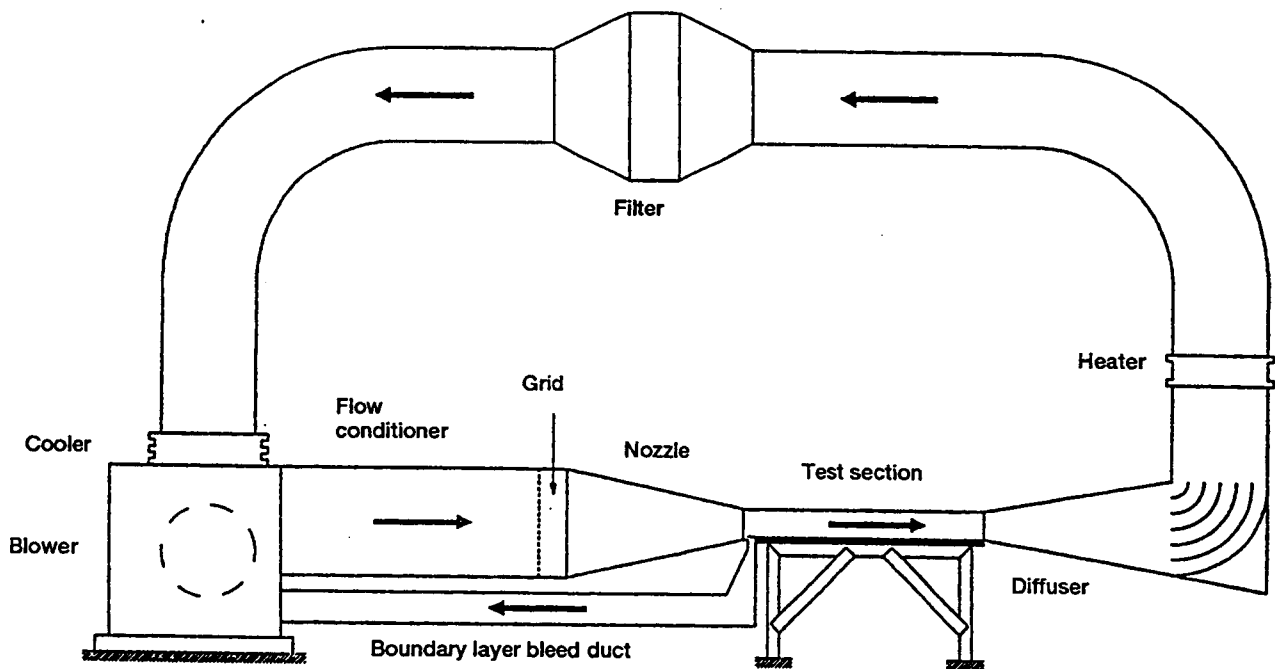


Figure 4.—Schematic diagram of the NASA/Lewis wind tunnel.

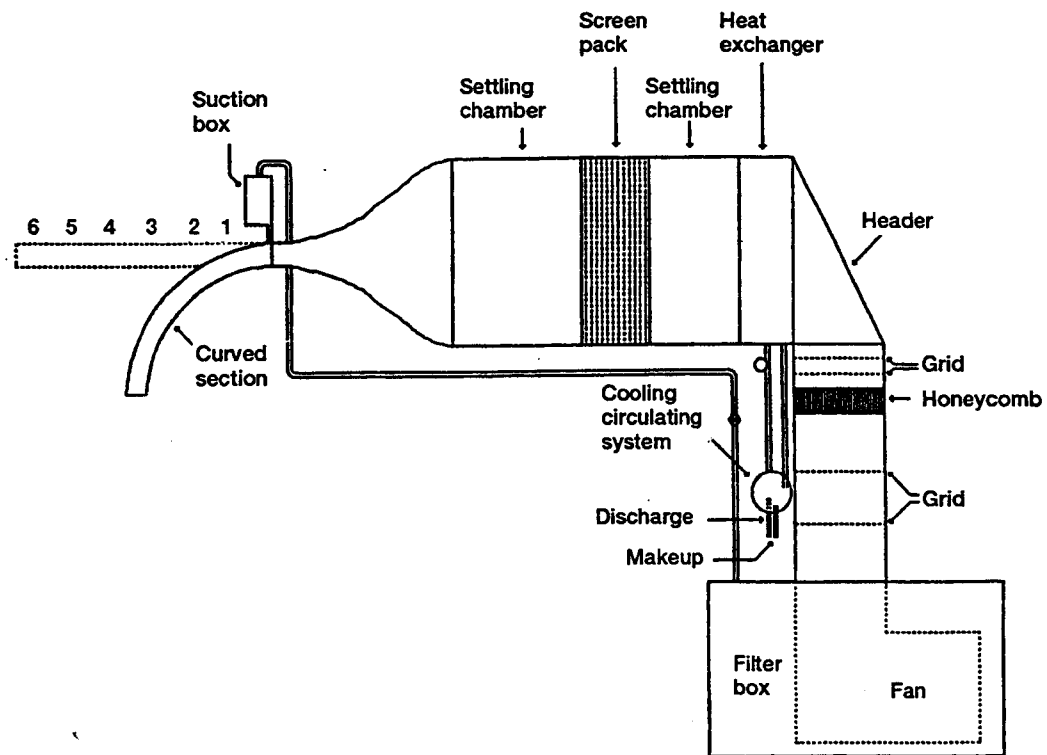
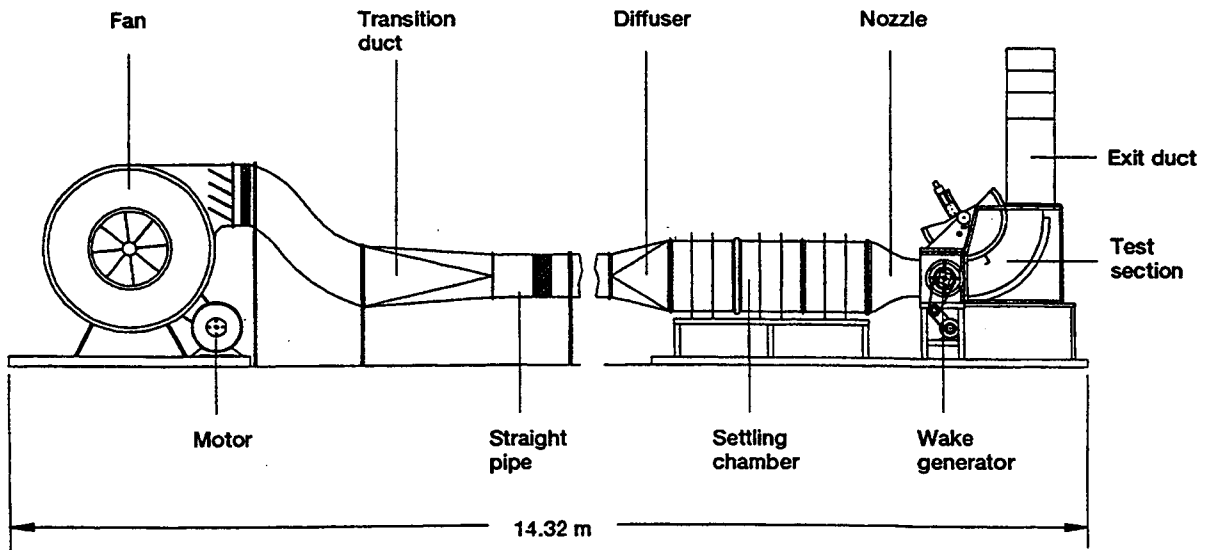
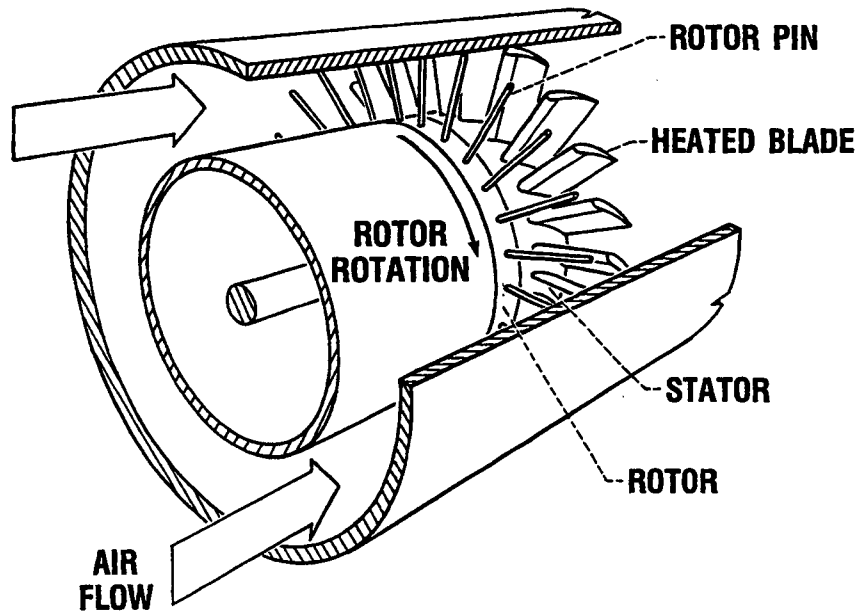


Figure 5.—Schematic diagram of the University of Minnesota test facility.



(a) Texas A&M "squirrel/cage" test facility.



(b) Rotor-wake heat transfer rig (NASA/Lewis).

Figure 6.—Rotor-wake test facilities.

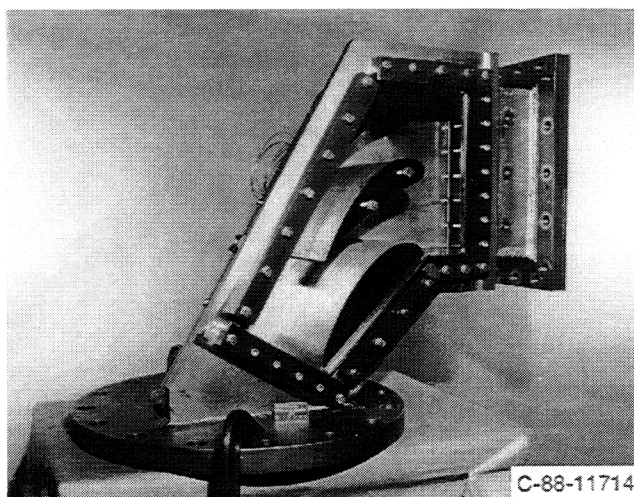
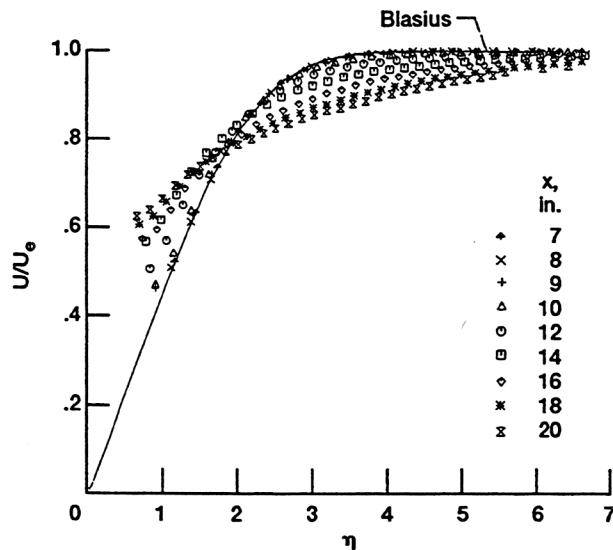
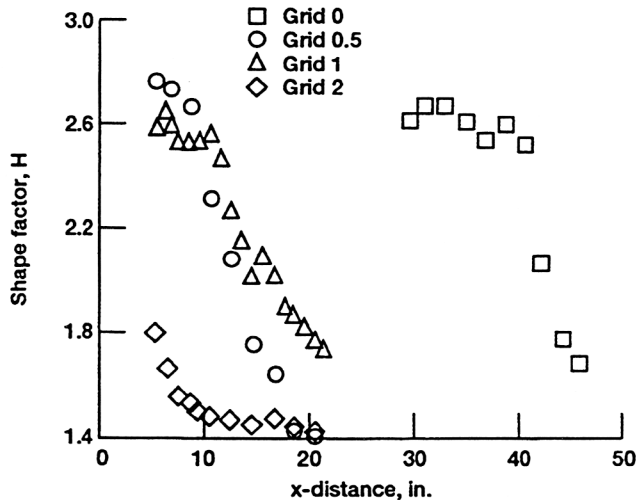


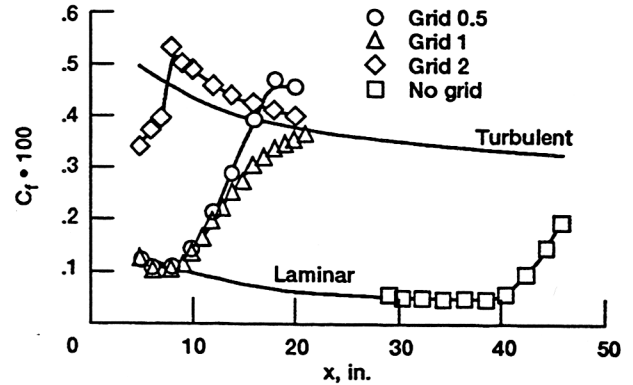
Figure 7.—Large blade test section (NASA/Lewis).



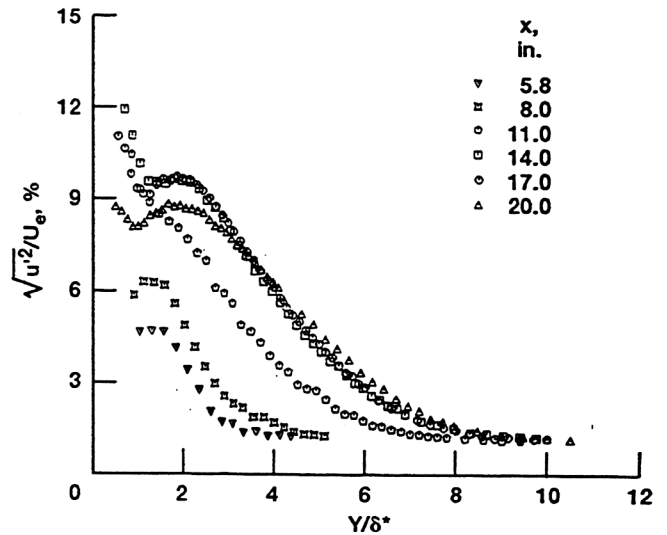
(a) Grid 1: plots of η versus $f(\eta)$ overlaid.



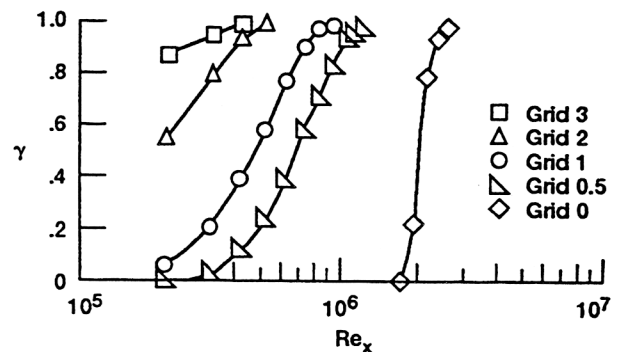
(b) Boundary layer shape factor versus x distance.



(c) Skin friction coefficient versus x distance.

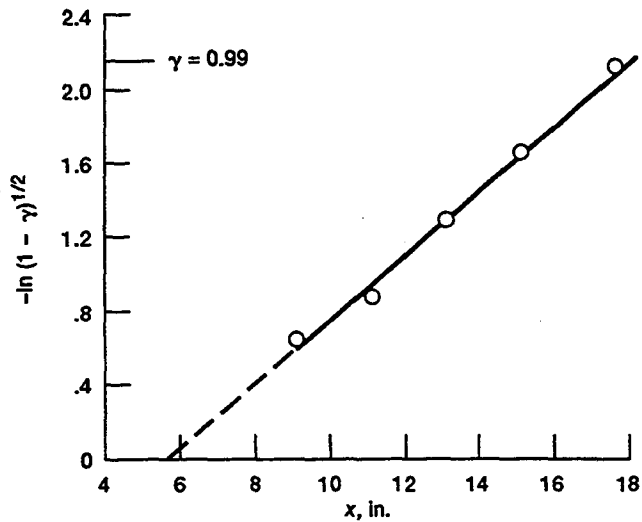


(d) Grid 1: Boundary layer profiles of the RMS of the velocity fluctuations within the boundary layer.

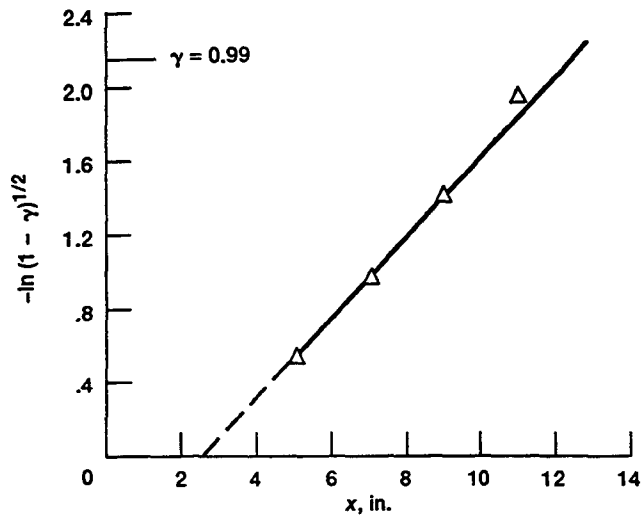


(e) Intermittency factor (γ) versus Reynolds number based on x distance.

Figure 8.—Experimental evidence of transition onset (Suder, O'Brien and Reshotko, 1988).



(a) Free-stream turbulence intensity, Tu_e , 1.1 percent: transition length, L_{tr} , 1.03 ft; nondimensional spot formation rate, 0.53×10^{-3} ; momentum thickness Reynolds number, $Re_{\theta, tr}$, 337.



(b) Free-stream turbulence intensity, Tu_e , 2.4 percent: transition length, L_{tr} , 0.81 ft; nondimensional spot formation rate, 0.26×10^{-3} ; momentum thickness Reynolds number, $Re_{\theta, tr}$, 229.

Figure 9.—Method of Narasimha (1957) for transition onset and length (Simon & Stephens, 1991).

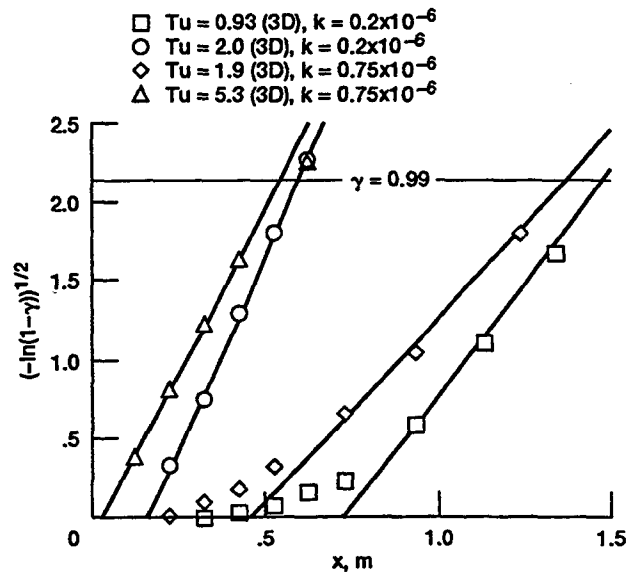


Figure 10.—Intermittency data for (data of Blair and Anderson, 1987) accelerated flow (Volino and Simon, 1991).

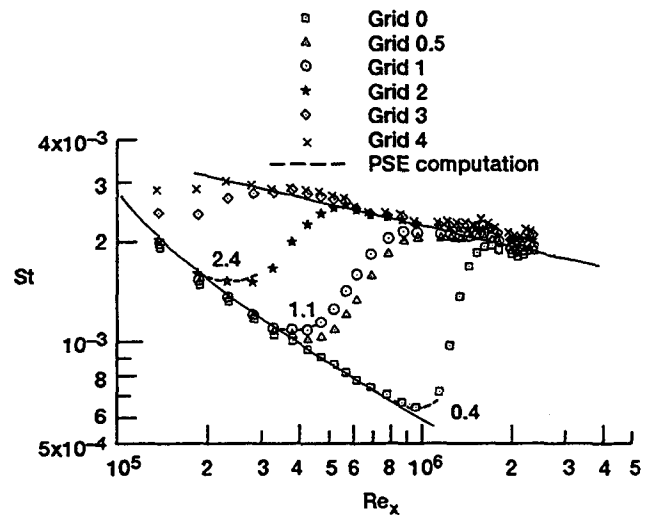


Figure 11.—Onset prediction using PSE approach (Stuckert & Herbert, 1992) Data of Sohn & Reshotko (1991).

- △ Kim (1990)
 - Sohn (1991)
 - Blair and Anderson (1987) $k = 0.2 \times 10^{-6}$
 - ◇ Blair and Anderson (1987) $k = 0.75 \times 10^{-6}$
- (1) Volino, Simon (1991) } Experiments

- MTS (2) Crawford
 - TXM (2) Crawford
 - Jones-Lauder (1) Simon, Stephens (1991)
 - ▲ Launder-Sharma (2) Sieger, Schulz, Crawford, Wittig (1992)
 - Nagano-Tagawa
 - ▼ K.Y. Chien
- } Computations

- (1) Based on intermittency
- (2) Based on minimum Stanton number

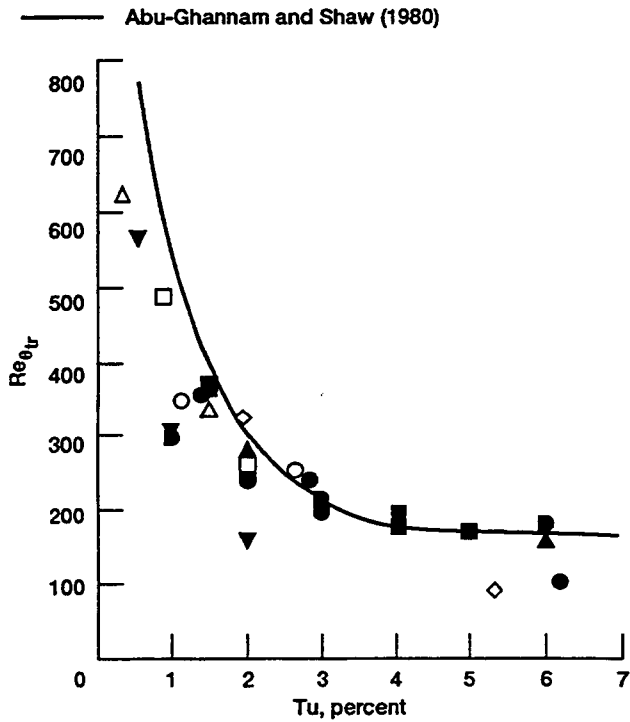


Figure 12.—Computed and experimental momentum thickness Reynolds number for transition onset.

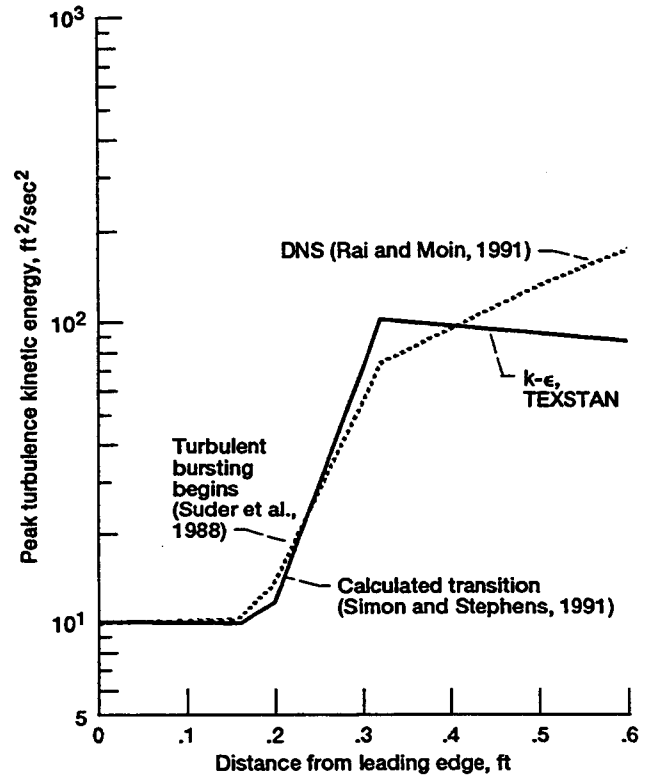


Figure 13.—Comparison of computed disturbance energy from computations based on a $k-\epsilon$ model and on direct numerical simulation (DNS) for bypass transition (Simoneau and Simon, 1993).

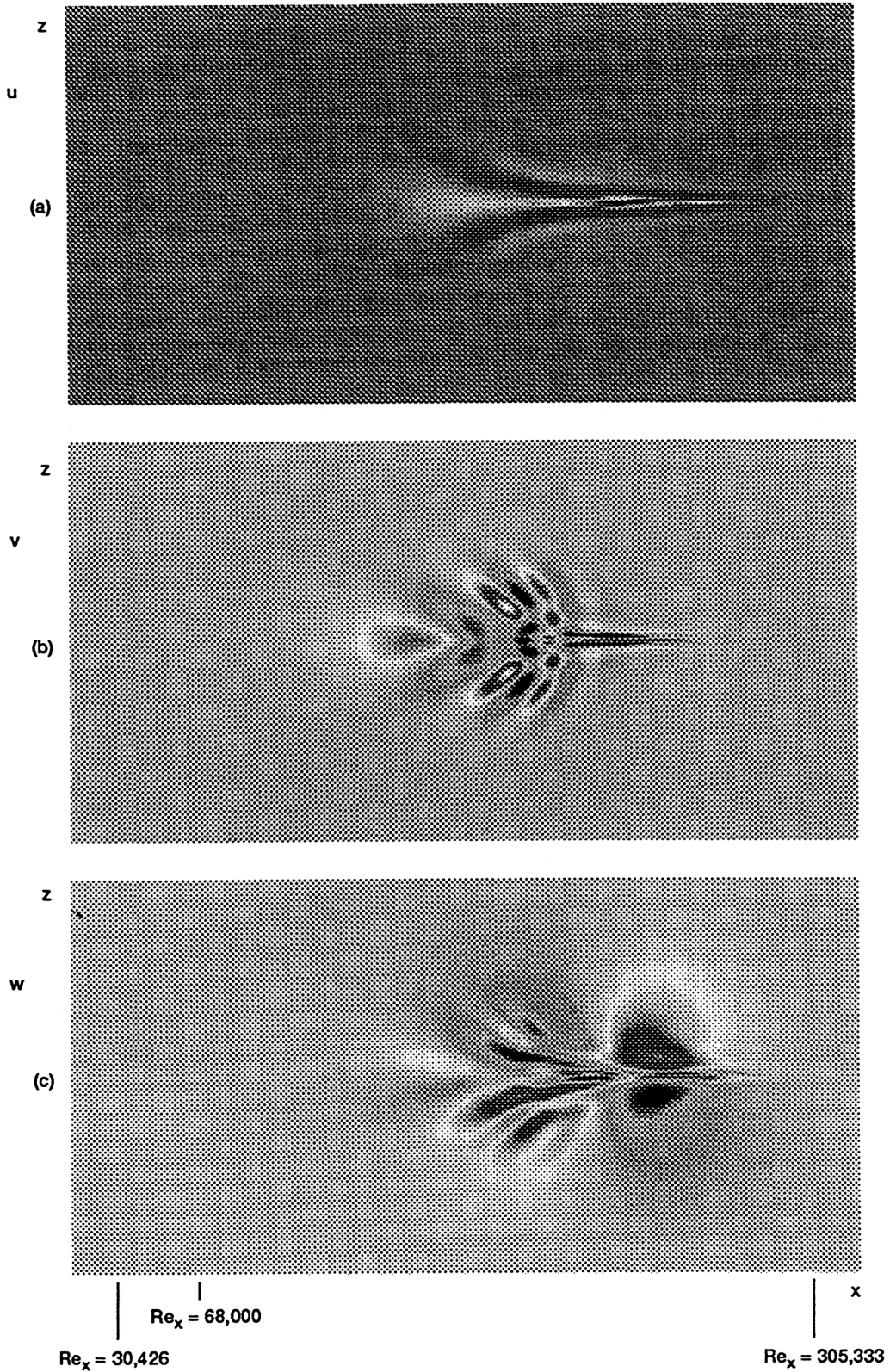


Figure 14.—Flow structure generated by a blowing pulse in Blasius boundary layer (Ashpis and Spalart, 1993) contours of velocity components are shown on a horizontal x-z plane at $y/\delta_0^* = 2.6$. The amplitude of the pulse is $0.01 U_e$. The pulse is generated at $Re_{x_0} = 68,000$ where displacement thickness $\delta_0^* = 1.112$, $Re_{\delta_0^*} = 448.7$.

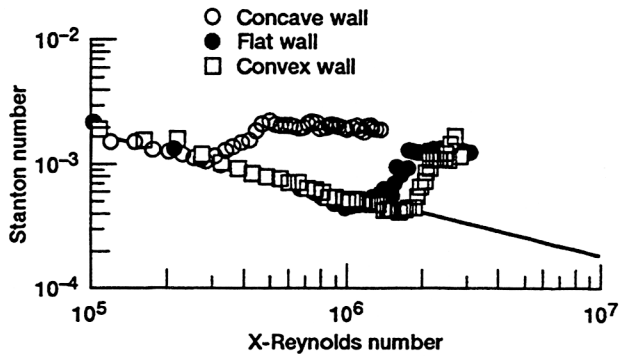


Figure 15.—Effect of streamwise curvature on bypass transition. Wall radii of curvature 90-100 CM; free-stream distribution level 0.6-0.7 percent. (Wang, 1984; Kim and Simon, 1991).

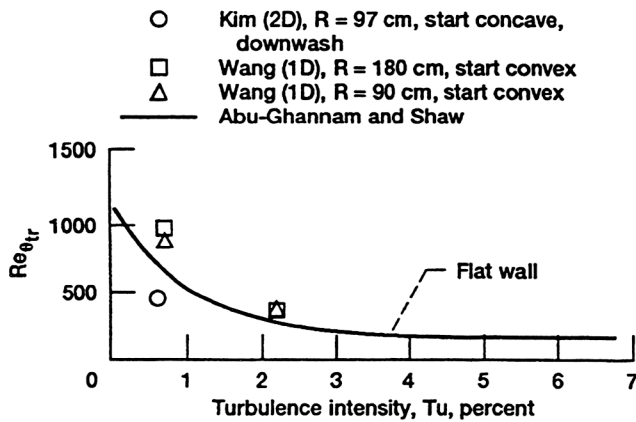
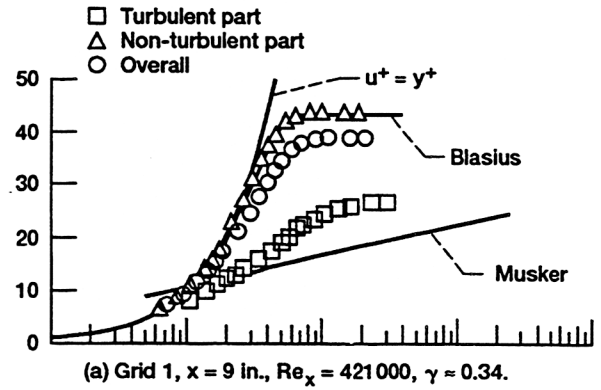
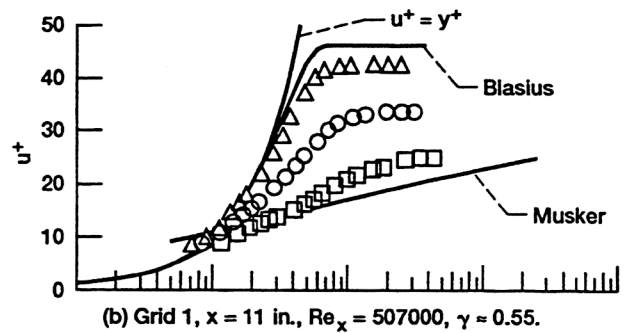


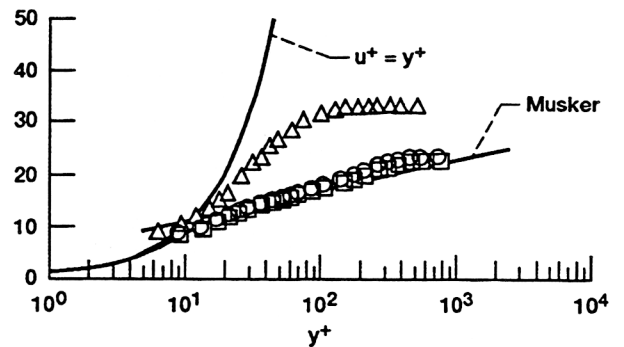
Figure 16.—Transition start based on St, curved wall cases. (Volino and Simon, 1991).



(a) Grid 1, $x = 9$ in., $Re_x = 421000$, $\gamma \approx 0.34$.



(b) Grid 1, $x = 11$ in., $Re_x = 507000$, $\gamma \approx 0.55$.



(c) Grid 1, $x = 17.5$ in., $Re_x = 841000$, $\gamma \approx 0.97$.

Figure 17.—Conditionally sampled mean velocity profiles in wall units. (Sohn, Reshotko and Zaman, 1991).

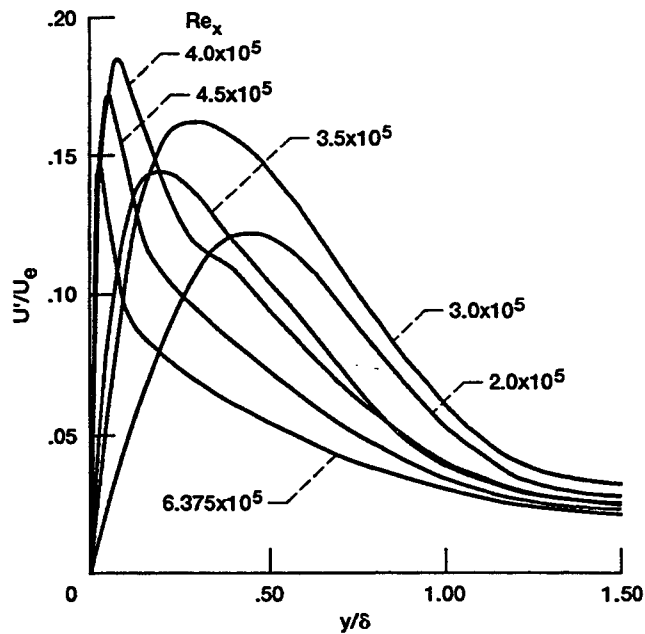


Figure 18.—DNS computed streamwise component of turbulence intensity (Rai and Moin, 1991).

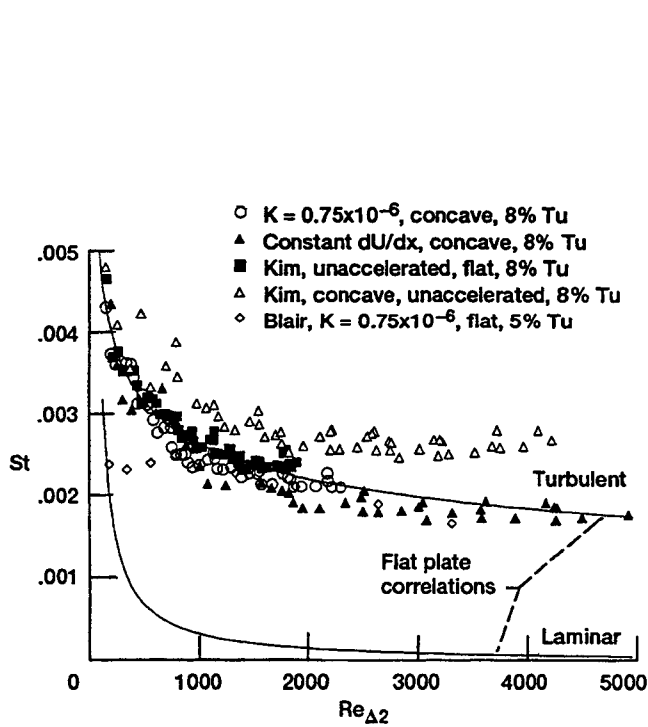


Figure 19.—Stanton numbers on concave and flat surfaces; unaccelerated and accelerated flow (Volino and Simon, 1993).

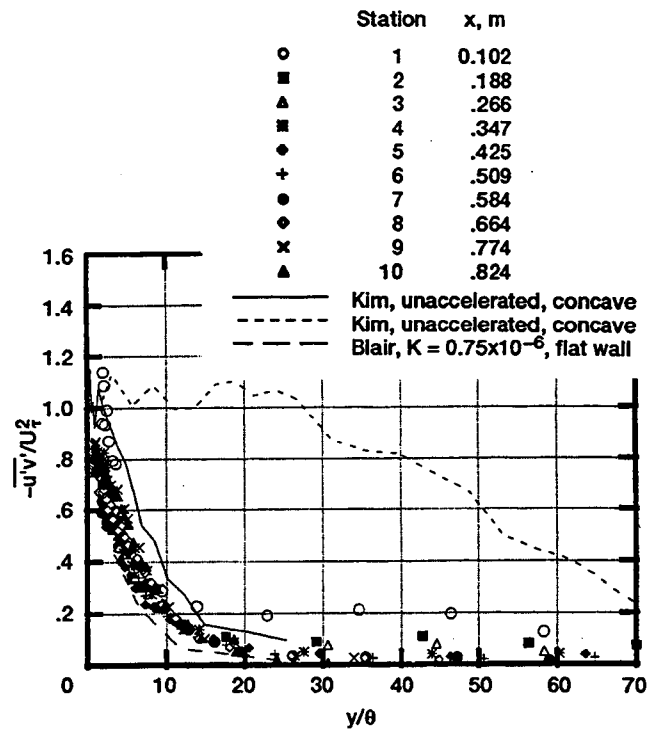


Figure 20.—Turbulent shear stress (concave surface), constant dU/dx case (Volino and Simon, 1993).

- △ Kim (1990)
 - Sohn (1991)
 - Blair and Anderson (1987) $k = 0.2 \times 10^{-6}$
 - ◇ Blair and Anderson (1987) $k = 0.75 \times 10^{-6}$
- (1) Volino, Simon (1991) } Experiments
- MTS (2) Crawford
 - TXM (2) Crawford
 - Jones-Launder (1) Simon, Stephens (1991)
- } Computations
- ▲ Launder-Sharma (2) Sieger, Schulz,
 - Nagano-Tagawa Crawford, Wittig
 - ▼ K.Y. Chien (1992)
- (1) Based on intermittency
(2) Based on minimum Stanton number

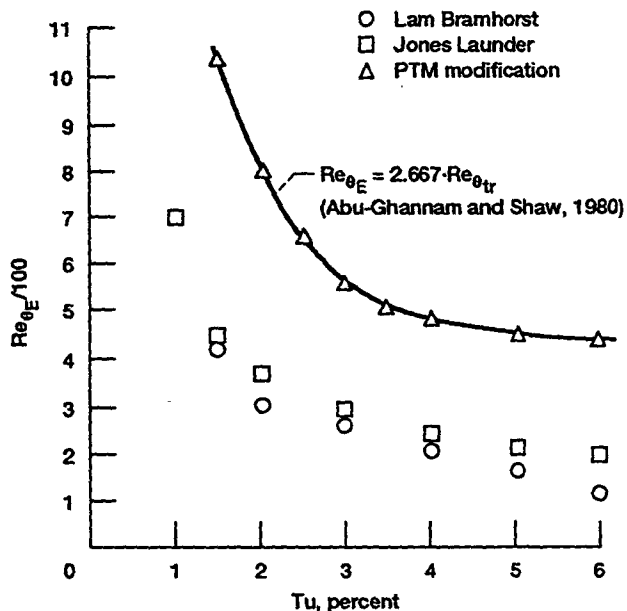


Figure 22.—Calculated momentum thickness Reynolds numbers at the end of transition using the "PTM" model (Schmidt and Patonkar, 1988).

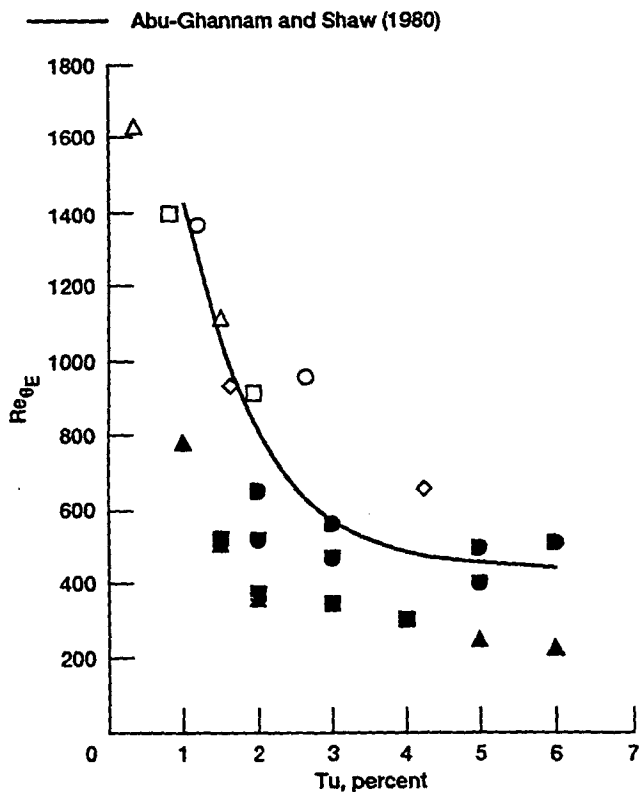


Figure 21.—Computed and experimental momentum thickness Reynolds number for transition onset.

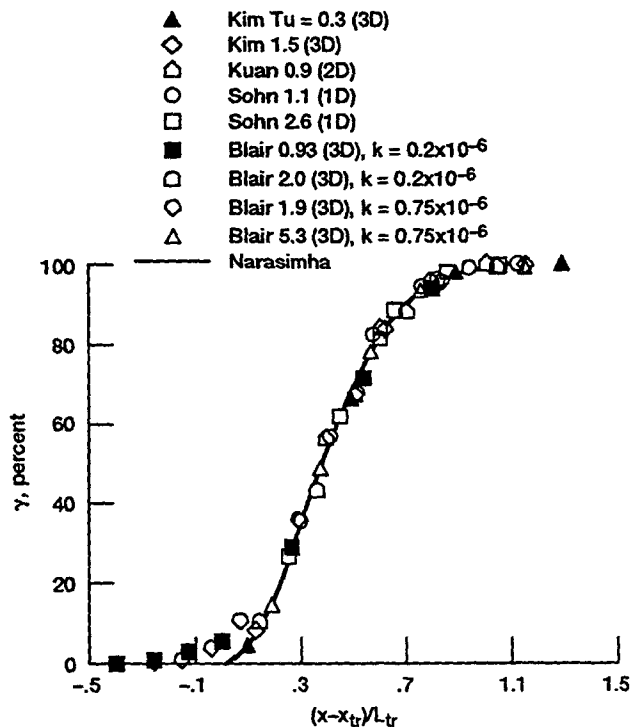


Figure 23.—Intermittency (Volino and Simon, 1991).

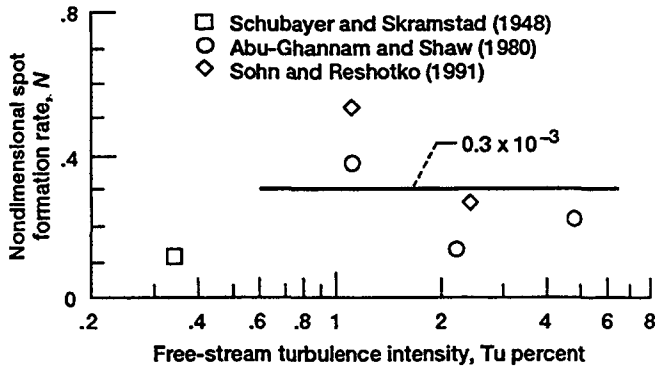


Figure 24.—Variation of nondimensional spot formation rate with free-stream turbulence (Narasimha (1985) method) (Simon and Stephens, 1991).

- △ Kim and Simon (1991)
 - Suder, et al. (1988)
 - Sohn and Reshotko (1991)
 - Blair and Anderson (1981) $k = 0.2 \times 10^{-6}$
 - Blair and Anderson (1987) $k = 0.75 \times 10^{-6}$
- $$k = \frac{\nu}{U_e^2} \frac{\partial U_e}{\partial X}$$

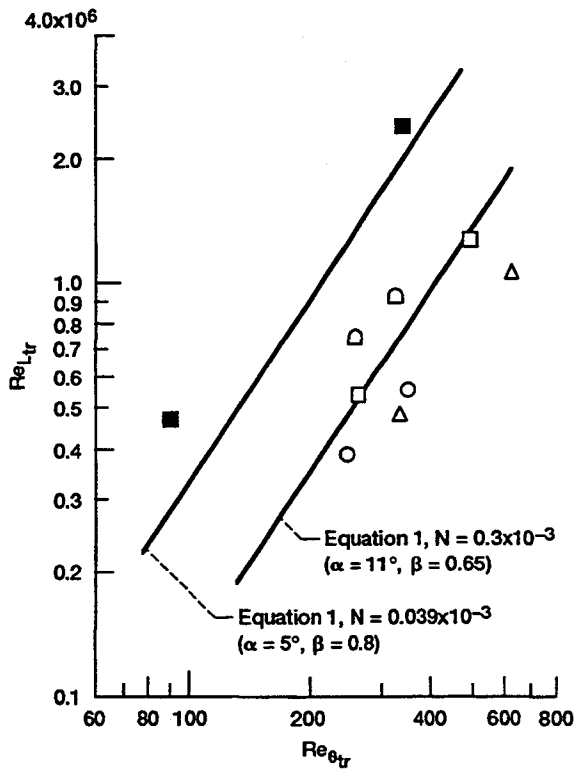


Figure 25.—Transition length correlation.

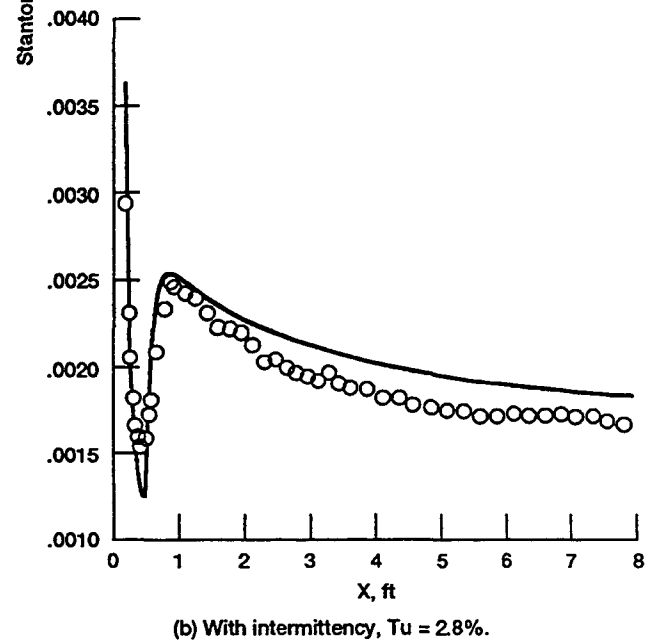
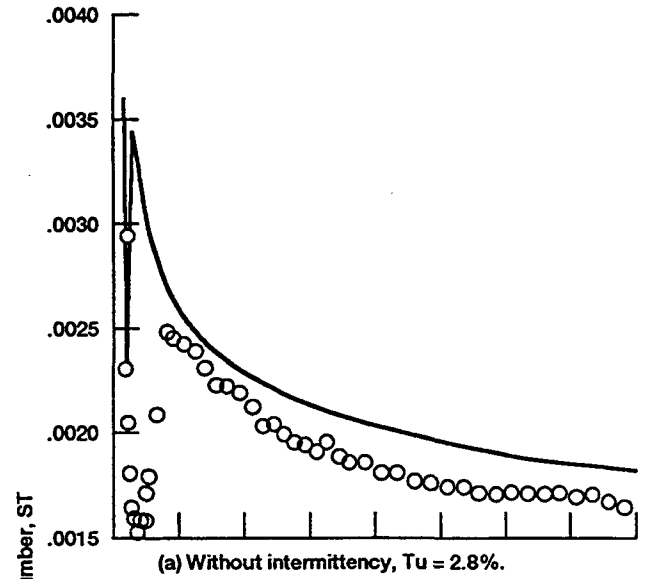


Figure 26.—Use of intermittency to model transition region.

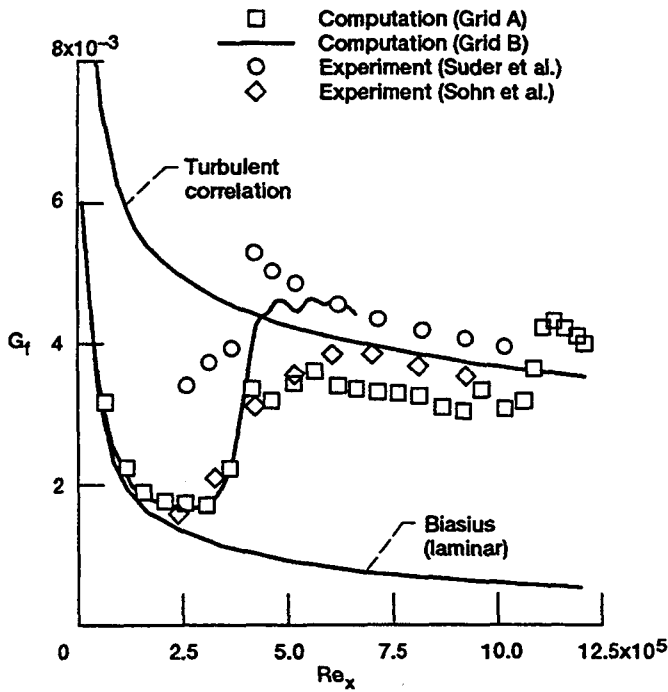


Figure 27.—Computed skin friction along the length of the flat plate (grids A and B). (Rai and Moin, 1991).

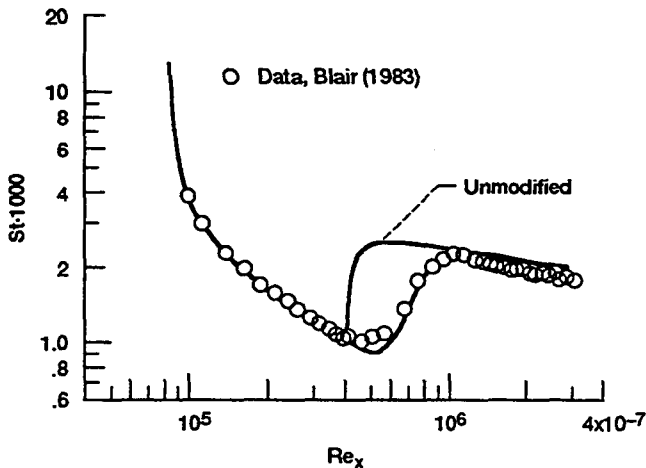
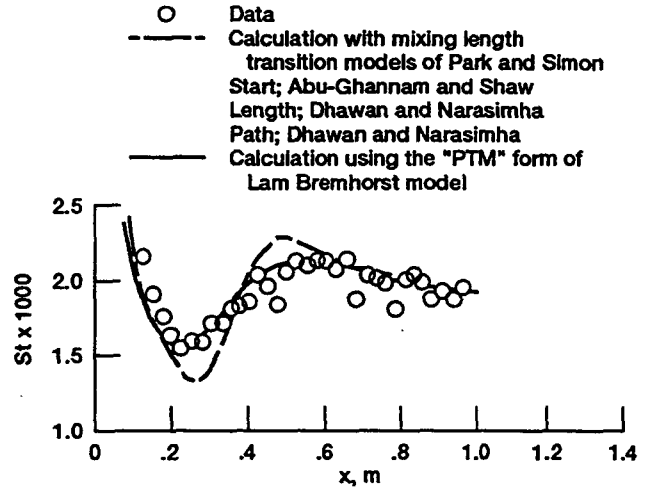
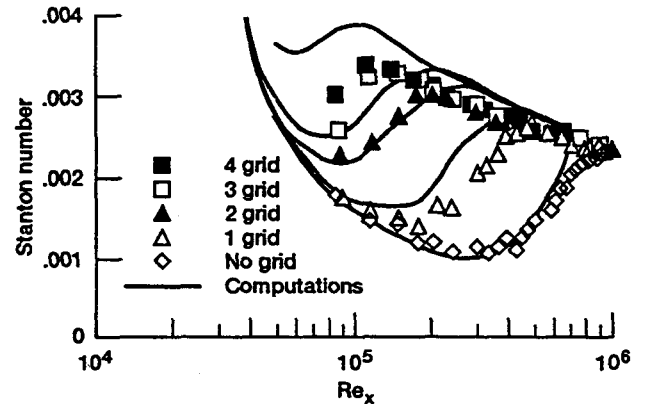


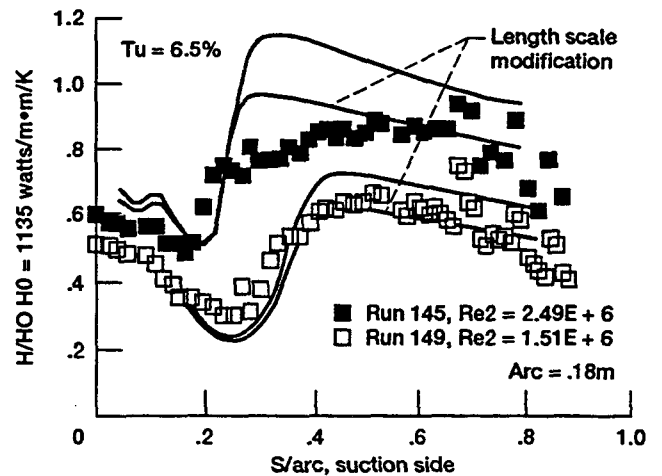
Figure 28.—Effect production term modification on the calculated Stanton number. $Tu = 1.4\%$ (Schmidt and Patankar, 1988).



(a) Comparison of the predicted heat transfer during transition with the data of Wang (1984).



(b) Comparison of the predicted heat transfer during transition with the zero pressure gradient data of Rued (1985) for k based on Tu .



(c) Comparison of the predicted and experimental heat transfer around the suction side of Hyllton et al.'s (1983) C3X blade.

Figure 29.—Computational results of PTM method (Schmidt and Patankar, 1988).

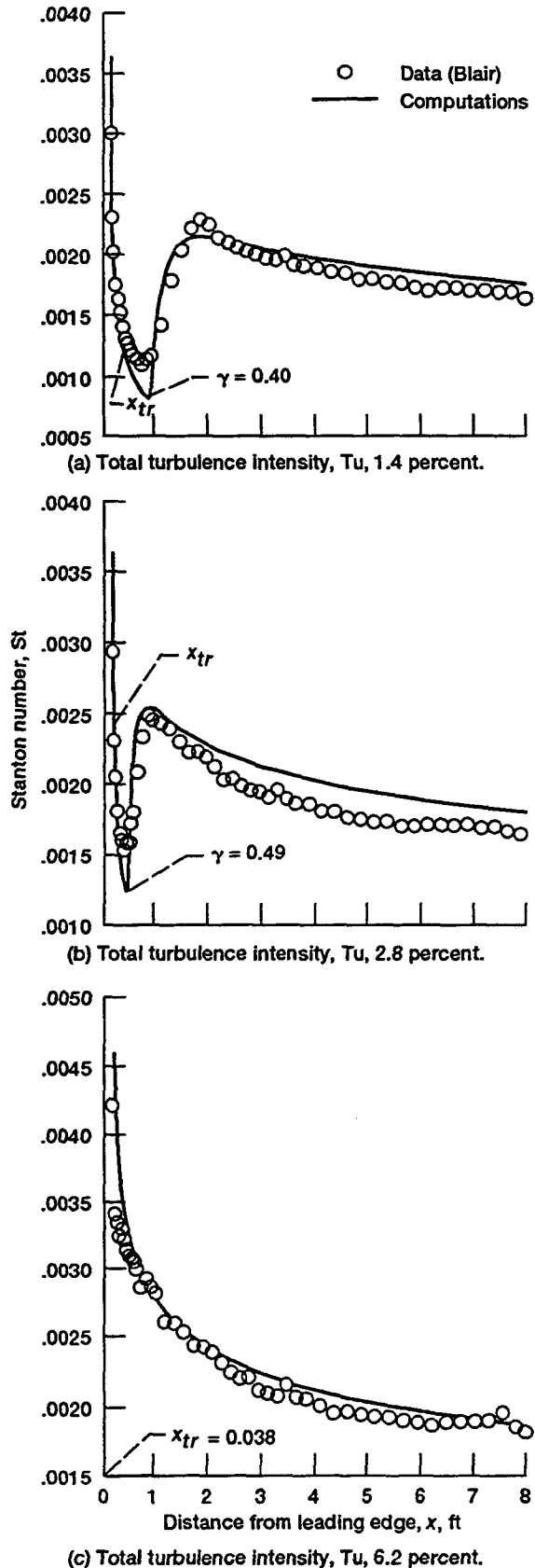


Figure 30.—Comparison of prediction with experiment (zero pressure gradient). (Simon & Stephens, 1991)

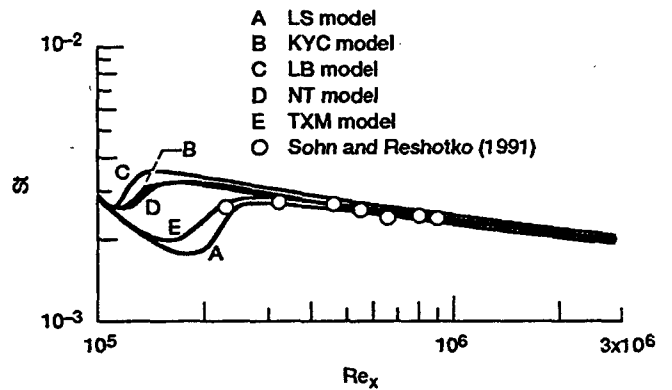


Figure 31.—The predictions of transition for flow over flat plate using different two-equation models compared with Sohn's data for grid 3 ($Tu = 3\%$) (Crawford, 1993).

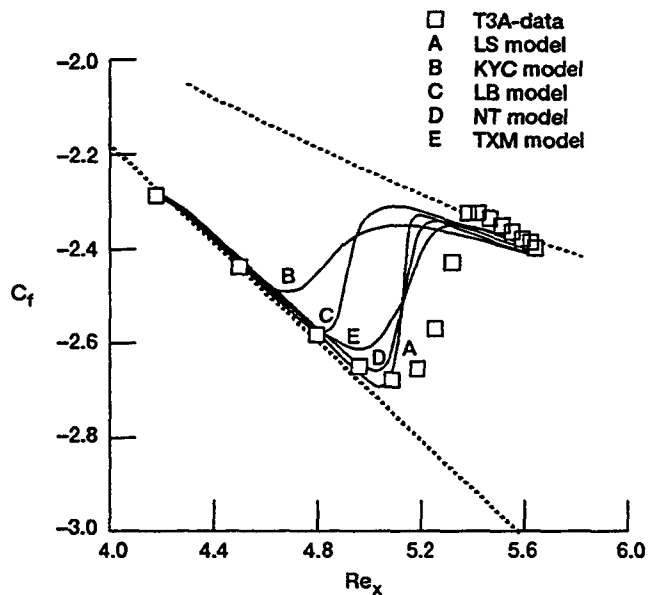


Figure 32.—Computational abilities of various turbulence models (Crawford, 1993). (T3A-data, Savill, 1991), $Tu = 3\%$ percent.

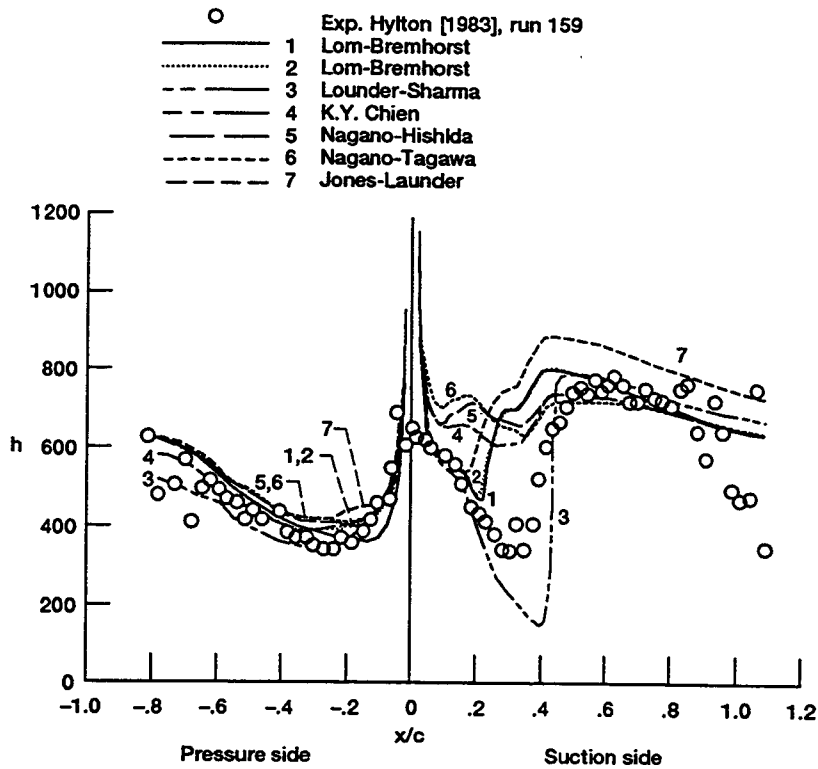


Figure 33.—Computational abilities of various turbulence models (Sieger, Schulz, Crawford and Wittig, 1992).

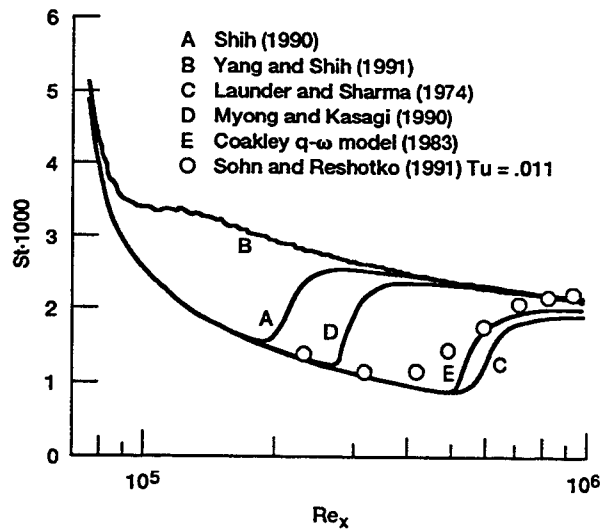


Figure 34.—Some computational comparisons with Sohn and Reshotko grid no. 1 (Wu and Reshotko, 1991).

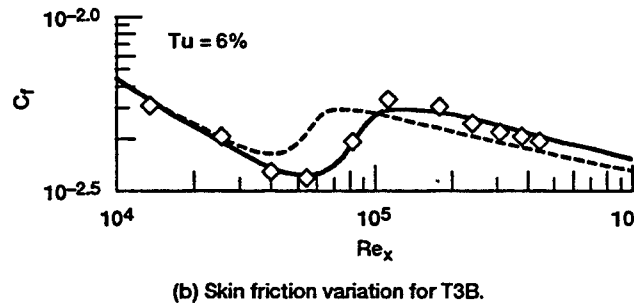
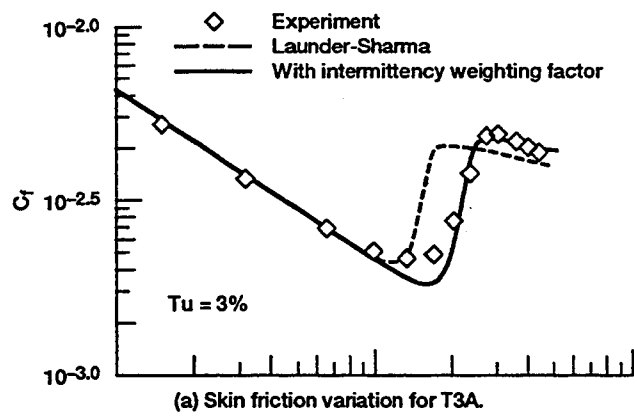


Figure 35.—Use of an intermittency weighting factor in computations (Yang, 1992; Yang and Shih, 1992).

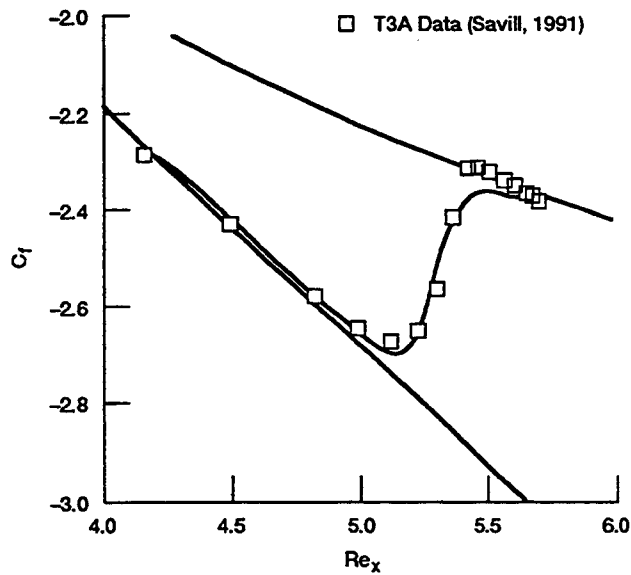


Figure 36.—The numerical prediction of transition flow using MTS model compared with experimental data of T3A (Crawford, 1993).

